© 2016. Published by The Company of Biologists Ltd | Development (2016) 143, 880-891 doi:10.1242/dev.129254

RESEARCH ARTICLE

The late and dual origin of cerebrospinal fluid-contacting neurons in the mouse spinal cord

Yanina L. Petracca[1,‡], Maria Micaela Sartoretti[1,‡], Daniela J. Di Bella[1], Antonia Marin-Burgin[2,*], Abel L. Carcagno[1], Alejandro F. Schinder[2] and Guillermo M. Lanuza[1,§]

ABSTRACT

Considerable progress has been made in understanding the mechanisms that control the production of specialized neuronal types. However, how the timing of differentiation contributes to neuronal diversity in the developing spinal cord is still a pending question. In this study, we show that cerebrospinal fluid-contacting neurons (CSF-cNs), an anatomically discrete cell type of the ependymal area, originate from surprisingly late neurogenic events in the ventral spinal cord. CSF-cNs are identified by the expression of the transcription factors Gata2 and Gata3, and the ionic channels Pkd2l1 and Pkd1l2. Contrasting with Gata2/3^{+} V2b interneurons, differentiation of CSF-cNs is independent of Foxn4 and takes place during advanced developmental stages previously assumed to be exclusively gliogenic. CSF-cNs are produced from two distinct dorsoventral regions of the mouse spinal cord. Most CSF-cNs derive from progenitors circumscribed to the late-p2 and the oligodendrogenic (pOL) domains, whereas a second subset of CSF-cNs arises from cells bordering the floor plate. The development of these two subgroups of CSF-cNs is differentially controlled by Pax6, they adopt separate locations around the postnatal central canal and they display electrophysiological differences. Our results highlight that spatiotemporal mechanisms are instrumental in creating neural cell diversity in the ventral spinal cord to produce distinct classes of interneurons, motoneurons, CSF-cNs, glial cells and ependymal cells.

KEY WORDS: Ependyma, Spinal cord, Central canal, Transcription factor, Late-born neurons

INTRODUCTION

Multipotent neural progenitor cells are responsible for the generation of the vast array of neuronal cell types found in the vertebrate nervous system, as well as astrocytes, oligodendrocytes and ependymal cells (Temple, 2001; Spassky et al., 2005; Rowitch and Kriegstein, 2010). Studies over the last two decades have revealed that positional identity is the main organizing principle initiating neuronal diversification. In the ventral neural tube, graded sonic hedgehog signaling activates transcriptional regulatory networks responsible for the interpretation of inductive signals and the subdivision of the neuroepithelium into five neural progenitor domains (designated pMN and p0-p3) (Briscoe et al., 2000; Balaskas et al., 2012; Lek et al., 2010). These dorsoventrally restricted progenitors produce distinct corresponding early-born classes of postmitotic neurons (motoneurons and V0-V3 interneurons) identified by the expression of specific sets of transcription factors (Jessell, 2000; Briscoe and Novitch, 2008; Goulding, 2009; Francius et al., 2013). As an example of further neuronal diversification, p2 progenitors generate several types of V2 interneurons, including excitatory V2a and V2d neurons, inhibitory V2b interneurons, which express the transcription factors Gata2 and Gata3, and V2c cells (Karunaratne et al., 2002; Li et al., 2005; Peng et al., 2007; Panayi et al., 2010; Panayiotou et al., 2013; Dougherty et al., 2013). Specification of V2 neuronal subtypes is determined by a mechanism involving Notch/Delta signaling and the transcription factors Foxn4, Tal1 and Lmo4 (Li et al., 2005; Peng et al., 2007; Del Barrio et al., 2007; Rocha et al., 2009; Batista et al., 2008; Kimura et al., 2008; Joshi et al., 2009).

The extent of neuronal subtype complexity found in the mature spinal cord suggests that, in addition to the spatial organization of progenitor domains, the timing of neurogenesis also plays determinant roles in neuronal diversification. Evidence of temporal developmental programs within restricted progenitor territories in the spinal cord includes dorsal Lbx1^{+} interneurons that are produced in consecutive neurogenic waves (Gross et al., 2002), and Renshaw cells, which constitute the earliest-born subset of V1 neurons (Stam et al., 2012; Sapir et al., 2004).

Despite our relatively deep knowledge about neuronal cell specification in the early developing neural tube, less attention has been paid to the existence of neurogenic events in the advanced embryonic spinal cord, in part because developmental stages beginning at embryonic day (E) 13.5 in the mouse have largely been considered exclusively gliogenic. During this period, after the decline in neurogenesis, neural tube progenitors are massively engaged in astrocytic and oligodendrocytic differentiation, in a regionally restricted manner (Zhou and Anderson, 2002; Lu et al., 2002; Hochstim et al., 2008; Tsai et al., 2012; Rowitch and Kriegstein, 2010).

In this study, we identify the genesis of a neuronal subtype during a time window previously assumed to be non-neurogenic. A novel subtype of Gata2/3-expressing neurons is generated in the mouse ventral spinal cord during unexpectedly advanced developmental stages. We recognized these late-born Gata2/3^{+} cells as cerebrospinal fluid-contacting neurons (CSF-cNs) (Vigh and Vigh-Teichmann, 1971; Vigh et al., 1977). CSF-cNs are an intriguing cell type located around the spinal central canal. CSF-cNs exhibit a peculiar morphology with a prominent dendritic extension through the ependymal layer terminating in a wide end bulb in the central canal (Vigh and Vigh-Teichmann, 1971, 1998; Vigh et al., 1983). More recently, CSF-cNs have been shown to

[1]Developmental Neurobiology Lab, Instituto Leloir and Consejo Nacional de Investigaciones Científicas y Técnicas (IIBBA-CONICET), Avenida Patricias Argentinas 435, Buenos Aires 1405, Argentina. [2]Neuronal Plasticity Lab, Instituto Leloir and Consejo Nacional de Investigaciones Científicas y Técnicas (IIBBA-CONICET), Avenida Patricias Argentinas 435, Buenos Aires 1405, Argentina.
*Present address: Instituto en Biomedicina de Buenos Aires, Partner Institute of the Max Planck Society (IBioBA-CONICET), Argentina.
‡These authors contributed equally to this work

§Author for correspondence (GLanuza@Leloir.org.ar)

Received 18 November 2015; Accepted 25 January 2016

Development (2016) 143, 880-891 doi:10.1242/dev.129254

express selectively the polycystic kidney disease 2-like 1 channel, Pkd2l1, which belongs to the transient receptor potential superfamily and has been proposed to serve mechano- and chemoreceptive functions (Huang et al., 2006; Djenoune et al., 2014; Orts-Del'Immagine et al., 2014). Although CSF-cNs were discovered a century ago and are present in all major groups of vertebrates, from cyclostomes to mammals (Vigh et al., 1983), their developmental origin and functions are only beginning to be unraveled.

We demonstrate that Gata2/3^{+}Pkd2l1^{+} cells do not belong to the Gata2/3^{+} V2b lineage or other early-born neuronal populations. We show that CSF-cNs derive from notably late progenitors positioned at two distinct dorsoventral coordinates: (1) the late p2 and dorsal half of pOL domains, and (2) the boundary between the p3 domain and the floor plate. Each of these sources produces a CSF-cN subset with distinct electrophysiological properties and conspicuous location surrounding the central canal. We thus provide strong evidence of neurogenic events in the late ventral neural tube that produce neurons of the central canal.

RESULTS

Spinal cord CSF-cNs are a subset of Gata2/3-expressing cells

Cell birthdate in the developing mouse neural tube was analyzed by pulse-chase 5-bromo-2′-deoxyuridine (BrdU) labeling. Timed pregnant mice were injected with BrdU once between E10.5 and E15.5 and the distribution of labeled cells was mapped in the postnatal day (P) 0 spinal cord (Fig. 1A,A′; Fig. S1A-F). Administration of BrdU between E10.5 and E12.5 marked neurons in the ventral and dorsal horns (Fig. 1A), whereas later BrdU applications labeled glial cells laterally migrating or in the white matter (Fig. 1A′). In addition, a group of cells in the proximity of the central canal proliferated between E13.5 and E15.5 (Fig. 1A′, cc).

In the spinal cord, the ependymal area surrounding the central canal comprises ependymocytes and several other cell types (Bruni, 1998; Meletis et al., 2008; Sabourin et al., 2009; Marichal et al., 2012). Cells located by the central canal, show a robust expression of the transcription factor Nkx6-1 (Fig. 1B), reflecting their ventral origin (Fu et al., 2003). We assessed the contribution of spinal V0-V3 populations to this region (Fig. 1C). V0 cells were identified at P0 by β-galactosidase in *Dbx1^{lacZ}* mice (Fig. 1D) (Pierani et al., 2001). V1, V2b and V3 neurons were traced using GFP conditional reporters in combination with *En1^{Cre}*, *Gata3^{Cre}* and *Sim1^{Cre}* alleles (Fig. 1E,G,H) (Sapir et al., 2004; Zhang et al., 2014, 2008), whereas V2a interneurons were detected by Chx10 (Vsx2 – Mouse Genome Informatics) staining (Fig. 1F). V0, V1, V2a and V3 cells were excluded from the ependymal area (Fig. 1D-H). By contrast, a subset of Gata3-derived cells was found around the central canal, when fate mapped with *Gata3^{Cre}* and GFP or tdTomato conditional reporters (Fig. 1G, arrow; Fig. S1G). Long-term genetic tracing in P14 *Gata3^{Cre};ZnG* mice recognized at least two groups of GFP^{+} cells in the spinal cord: interneurons located laterally in lamina VII (Fig. 1I, arrowhead) (Zhang et al., 2014; Lundfald et al., 2007), and a second group in the vicinity of the central canal (Fig. 1I, arrow).

In the postnatal ependymal area, Gata3-derived cells comprise 28±5% (mean±s.d.) of Nkx6-1^{+} cells (Fig. S1G,H) and display morphological heterogeneity (Fig. S1J-N). To characterize these cells further, we assessed the presence of Gata2, which is usually co-expressed with Gata3. Using the *Gata2^{GFP}* line (Fig. S1I,O-T), we found that 60.5±6.3% of tdTomato^{+} central canal cells in *Gata3^{Cre};tdTomato* mice express Gata2 (Fig. S1G,H). Strikingly, at both P0 and P14, Gata2 distinguished a group of central canal cells with homogeneous morphology (Fig. 1J-M; Fig. S1J-N). Whole-cell GFP labeling identified these cells as the cerebrospinal fluid-contacting neurons of the central canal (CSF-cNs) (Vigh and Vigh-Teichmann, 1971, 1998; Vigh et al., 1977; Stoeckel et al., 2003; Marichal et al., 2009) (Fig. 1J-M). These cells exhibit a unique morphology, with a process into the central canal contacting the cerebrospinal fluid (Fig. 1K,K′,M, arrows). In addition, CSF-cNs exclusively express Pkd2l1, which, together with Gata2, unequivocally identifies this cell type in the ependymal region (Fig. 1J-M; Fig. S1N).

Pkd2l1^{+}Gata2^{+} cells are present both in the lateral (Fig. 1K) and ventral (Fig. 1K′) regions of the central canal. Those settled in

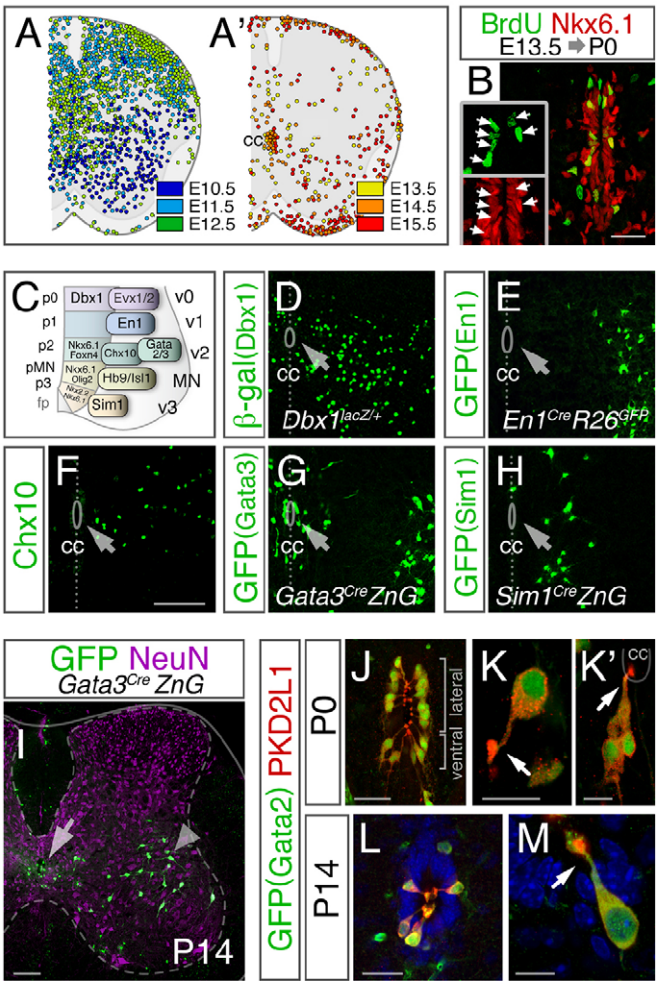

Fig. 1. A subset of Gata2/3^{+} cells surrounds the central canal of the spinal cord. (A,A′) Distribution of BrdU-labeled cells at P0 after one pulse at E10.5-E15.5. (B) A single BrdU pulse at E13.5 marked Nkx6-1^{+} cells around the P0 central canal. Arrows in insets indicate Nkx6-1^{+}BrdU^{+} cells. (C-H) Contribution of spinal V0-V3 cells to the central canal region. (C) Scheme of ventral progenitor domains and neurons. (D-H) P0 spinal cord sections stained for β-galactosidase (D; *Dbx1$^{lacZ/+}$*), GFP (E; *En1^{Cre};R26^{GFP}*), Chx10 (F), GFP (G; *Gata3^{Cre};ZnG*) and GFP (H; *Sim1^{Cre};ZnG*). GFP in Gata3-derived cells labels V2b interneurons in the ventrolateral spinal cord and a novel subgroup at the ependymal area (G). Arrows indicate the presence (G) or absence (D-F,H) of labeled cells by the central canal. Dotted line indicates the midline. (I) Fate mapping in P14 *Gata3^{Cre};ZnG* shows cells by the central canal (arrow) and lamina VII interneurons (arrowhead). NeuN staining delineates the gray matter (outlined by dashed line). (J-M) Co-expression of Pkd2l1 and Gata2 (GFP, *Gata2^{GFP}*) around the P0 and P14 central canal. GFP^{+}Pkd2l1^{+} cells located laterally (K) or ventrally (K′) to the central canal with their processes contacting the CSF (K,K′,M, arrow). Blue, DAPI counterstain. Scale bars: 100 µm in D-I; 30 µm in B,J,L; 10 µm in K,K′,M. See also Fig. S1. cc, central canal; fp, floor plate.

Development (2016) 143, 880-891 doi:10.1242/dev.129254

the lateral wall account for 73±6% of CSF-cNs at P0 (Fig. 1J,K; 12.8±2.8 cells per section), and the rest are located by the ventral midline of the spinal cord (Fig. 1J,K′; 5.3±1.6 cells/section, 27±6% of CSF-cNs). Although the somas of CSF-cNs in the ventral quadrant are further from the central canal, they also contain a process contacting the CSF (Fig. 1K′, arrow).

Gata2^{+} CSF-cNs are immature neurons

Although spinal CSF-cNs have been described in a wide number of vertebrate species (Vigh and Vigh-Teichmann, 1971; Vigh et al., 1977, 1983; Stoeckel et al., 2003; Marichal et al., 2009; Huang et al., 2006; Djenoune et al., 2014; Jalalvand et al., 2014), their characteristics remain to be fully clarified. We evaluated the expression of distinct cellular markers and found that CSF-cNs express high levels of Nkx6-1 and Sox2 (Fig. 2A,B), which are usually downregulated upon neuronal differentiation (Bylund et al., 2003). Pkd2l1-expressing cells are positive for neuronal β-III-tubulin (Fig. 2C) and doublecortin (Dcx; Fig. 2C′) but do not express NeuN (Rbfox3 – Mouse Genome Informatics) (Fig. 2D), suggesting that Pkd2l1^{+} cells comprise an immature neuronal population. This expression pattern is maintained postnatally, as shown at P14 (Fig. S2A-D). Accordingly, there is no colocalization between Pkd2l1 and the astrocytic marker Gfap or between Pkd2l1 and vimentin, which characterizes ependymocytes (Fig. 2E,F).

In common with CSF-cNs in lamprey, fish, amphibian and other mammals (Barber et al., 1982; Dale et al., 1987b; Stoeckel et al., 2003; Jalalvand et al., 2014; Djenoune et al., 2014), CSF-cNs are mainly GABAergic, with ∼80% of Pkd2l1^{+} cells at P0 labeled by GFP in *Gad1*^{GFP} mice (Fig. 2G). In addition, *in situ* hybridizations for the genes encoding the vesicular GABA transporter vGAT (Slc32a1 – Mouse Genome Informatics), Gad1 and Gad2, but not for glutamatergic and cholinergic markers, detected CSF-cNs at the P14 central canal (Fig. S2E-I). Contrasting with CSF-cNs in lamprey (Jalalvand et al., 2014), mouse CSF-cNs do not produce somatostatin, as assessed in *Sst*^{Cre}*;td-tomato* mice (Fig. S2J).

In several cellular systems, Pkd2 channel activity depends on physical interactions with members of the polycystin-1 family to form receptor-channel complexes (Semmo et al., 2014; Ishimaru et al., 2006). Searching for potential partners of Pkd2l1 in CSF-cNs, we discovered that Pkd1l2 is expressed with a pattern similar to Pkd2l1 (Fig. 2H). Notably, by combined *in situ* hybridization and antibody staining, we demonstrated the co-expression of Pkd1l2 and Pkd2l1 (Fig. 2H, inset), suggesting that they are assembling partners in CSF-cNs.

We next determined the electrophysiological properties of CSF-cNs by whole-cell patch-clamp recordings in P1-P2 *Gata2*^{GFP} acute spinal cord slices (Fig. 1J-K′; Fig. 2I). Membrane excitability of central canal GFP^{+} cells was revealed by voltage-dependent fast

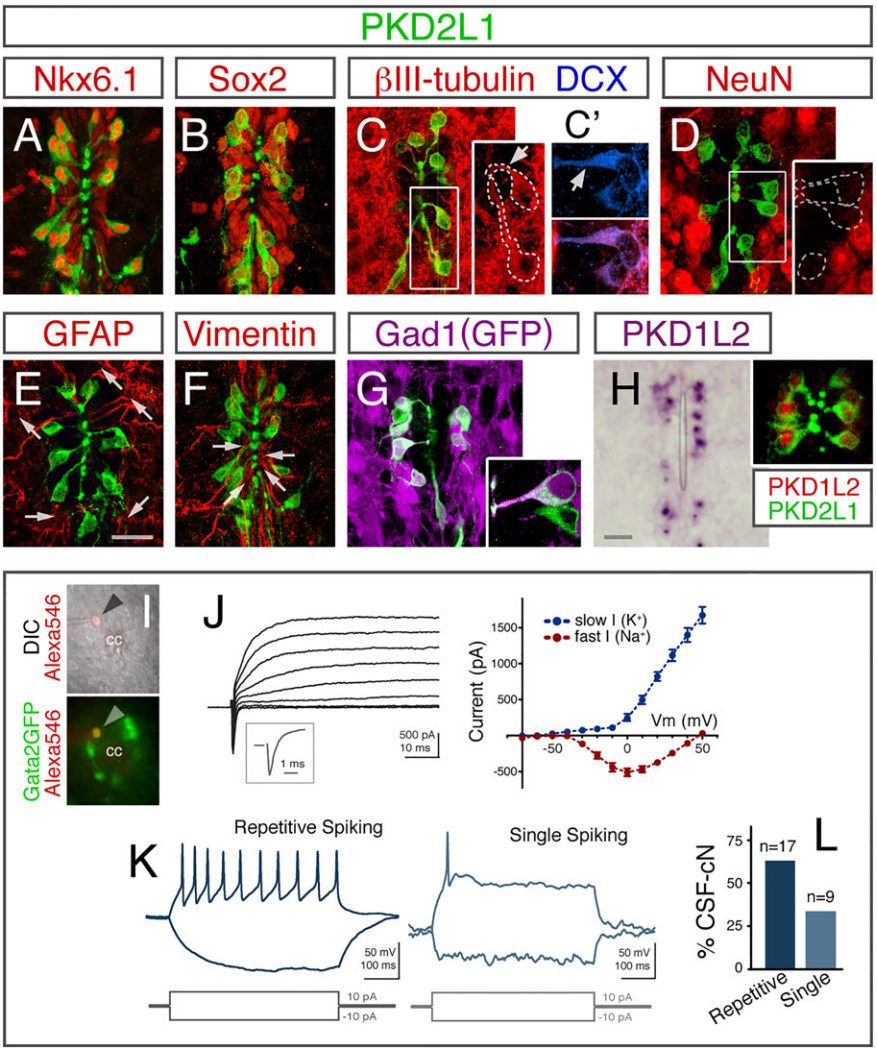

Fig. 2. Gata2^{+} CSF-cNs are immature neurons. (A-H) P0 central canal immunostained for Pkd2l1 and Nkx6-1, Sox2, βIII-tubulin, NeuN, Gfap or vimentin (A-F). CSF-cNs express Sox2, Nkx6-1, neuronal βIII-tubulin (see processes into the cc, outlined in C inset) and Dcx but are negative for NeuN, Gfap or vimentin. Arrows in C,C' point to βIII-tubulin^{+}DCX^{+} processes. The majority of CSF-cNs are marked in *Gad1*^{GFP} mice (G); inset shows both Gad1-positive and -negative CSF-cNs. (H) *In situ* hybridization against *Pkd1l2*. Inset shows *Pkd1l2* mRNA in combination with an anti-Pkd2l1 antibody. Scale bars: 30 µm. Arrows in E and F point to astrocytes and ependymocytes. (I-L) Electrophysiological recordings of GFP^{+} CSF-cNs in P1-P2 spinal cord acute slices. (I) GFP^{+} neuron labeled with Alexa Fluor 546 through the patch pipette. Arrowheads indicate pipette tip. (J) Left panel: depolarizing voltage steps (−60 mV to +10 mV) elicited fast inward (inset) and slow outward currents. Right panel: current-voltage plot of the peak inward and steady-state outward currents. Data are mean±s.e.m. (n=19 GFP^{+} cells). (K,L) Representative membrane potential recordings elicited by depolarizing current steps (10 pA, 0.5 s). Two different firing patterns were found: repetitive (n=17/26) and single spikes (n=9/26). No mixed patterns were found. See also Fig. S2. cc, central canal.

Development (2016) 143, 880-891 doi:10.1242/dev.129254

inward and delayed outward currents, measured under voltage-clamp configuration (Fig. 2J). GFP$^+$ cells generate action potentials in response to depolarizing steps in current-clamp (Fig. 2K; n=26/26); 66% of them elicit repetitive spiking with limited adaptation, and the remaining 34% display single spikes (Fig. 2K,L). Furthermore, CSF-cNs have a high input resistance (R_{in}=5.5±0.5 GΩ; n=25), a feature of neuronal immaturity (Ziskind-Conhaim, 1988; Zhang, 2004; Espósito et al., 2005). Altogether, the molecular and physiological characterization demonstrates that Gata2$^+$ central canal cells are excitable immature neurons.

CSF-cNs are late-born spinal cells

Because CSF-cNs express Gata2 and Gata3, which have been considered to reflect V2b neuronal identity (Karunaratne et al., 2002; Peng et al., 2007; Lundfald et al., 2007; Li et al., 2005), we investigated whether CSF-cNs belong to the V2b population or comprise a different group sharing the expression of these transcription factors. Previous studies have shown that V2b interneurons differentiate between E10 and E12 in the mouse neural tube (Karunaratne et al., 2002; Peng et al., 2007; Li et al., 2005; Zhou et al., 2000; Francius et al., 2013) (Fig. S3G-K′). To establish when CSF-cNs develop, we examined the time course of Pkd2l1 expression (Fig. 3A-D). The first Pkd2l1$^+$ cells were found at E14.5 and as development proceeds the number increases, then remains constant after E16.5 (Fig. 3A-D; ∼20 cells/section). Immunohistochemistry against Gata2 (Fig. 3E,F) or GFP in *Gata2^{GFP}* mice (Fig. 3G,H) revealed that the appearance of Pkd2l1 is coincident with the onset of Gata2 in these cells and that Pkd2l1 is always co-expressed with Gata2 (Fig. 3E-H; 99%). The timing of Pkd2l1 expression was assessed also in the chick spinal cord. We found that, similarly to the mouse, Pkd2l1 appears at advanced embryonic stages in the chick (Fig. S3A-F, >stage32).

The late onset of Pkd2l1 and Gata2 expression might reflect a delayed differentiation step of postmitotic cells generated earlier, or the birth of CSF-cNs at advanced stages (as suggested by Fig. 1A). Aiming to discriminate between these possibilities, BrdU was administered to pregnant females to cover different time windows, and the number of BrdU$^+$Pkd2l1$^+$ cells was assessed at E15.5 (Fig. S3M-O). Consistent with CSF-cNs being postmitotic, no Pkd2l1$^+$ cells incorporated BrdU when it was applied 12 h before analysis and only a small proportion was labeled when BrdU was administered 24 h prior to the analysis (E14.5-E15 pulse; Fig. S3N, O). The administration of BrdU at E13-E13.5 or E13.5-E14 rendered 39-44% of Pkd2l1-expressing cells BrdU$^+$ (Fig. S3M-O), interestingly indicating that CSF-cNs progenitors still divide at ∼E13. To confirm CSF-cNs birthdate, pregnant females were pulsed with BrdU for 24 h beginning at E13 or E16, and the spinal cords of P0 offspring were analyzed (Fig. 3I-K). The majority of CSF-cNs incorporated BrdU between E13 and E14 (∼70% of Pkd2l1$^+$ cells; Fig. 3I,I′,K), but only a minor proportion was positive when BrdU was applied at E16-E17 (Fig. 3J,J′,K).

This ‘late’ developmental stage has been assumed to be non-neurogenic in the ventral spinal cord, but exclusively gliogenic (Rowitch and Kriegstein, 2010; Altman and Bayer, 1984; Rowitch, 2004). Accordingly, we found that the first cohort of Gata2$^+$Pkd2l1$^+$ neurons at E14.5 appears together with astrocyte and oligodendrocyte differentiation, as revealed by cells expressing Sox9, Nfia or Olig2 migrating outside the spinal cord ventricular zone (Fig. 3L-N).

In summary, these results show that CSF-cNs progenitors divide after E13, and demonstrate that birthdate distinguishes two different groups of spinal Gata2/3-expressing neurons: (1) lamina VII V2b neurons, produced between E10 and E12 (Fig. S3G-I), and (2) CSF-cNs generated at ∼E14, a surprisingly late developmental stage for neurogenesis.

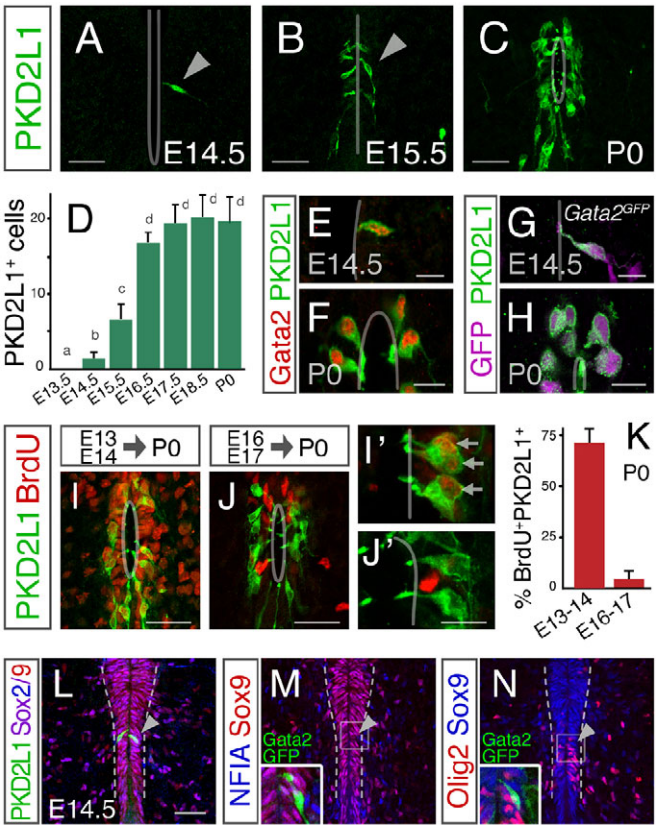

Fig. 3. CSF-cNs are Gata2$^+$ late-born spinal cells. (A-D) Pkd2l1 expression in E14.5, E15.5 and P0 spinal cord sections and quantification of Pkd2l1$^+$ cells (n=3-10 animals each). Arrowheads indicate Pkd2l1$^+$ cells. Letters indicate statistical significance (P<0.001, Kruskal–Wallis with post-hoc Dunn’s test) (groups with different letters are significantly different from one another). (E-H) Pkd2l1$^+$ cells (1389/1409) express Gata2 at E14.5 and P0, as shown by immunohistochemistry (E,F) or in *Gata2^{GFP}* mice (G,H). (I-K) Birthdate analysis of CSF-cNs. BrdU was applied for 24 h (pulsed every 4 h) during E13-E14 (I,I′) or E16-E17 (J,J′), and analyzed at P0. Arrows indicate Brdu$^+$Pkd2l1$^+$ cells. (K) Percentage of Pkd2l1$^+$ cells labeled with BrdU (27 sections, 3 pups each). (L-N) CSF-cNs arise along with glial cells. At E14.5, when Pkd2l1$^+$Gata2$^+$ CSF-cNs begin to appear (arrowheads, insets), astrocyte precursors outside the ventricular zone (dashed line) are identified by Sox2 and Sox9 (L) or Nfia and Sox9 (M) expression. Migrating oligodendrocytes were identified by Olig2 (N). Bars are mean±s.d. Scale bars: 30 µm in A-C,I,J, L-N; 10 µm in E-H,I′,J′. See also Fig. S3. Gray line indicates position of the ventricle or the central canal in A-C,E-H,I-J′.

Foxn4 controls early-born Gata2$^+$ V2b neurons but is dispensable for Gata2$^+$ CSF-cN development

Our findings demonstrate that V2b and CSF-cNs are early- and late-born Gata2/3$^+$ spinal cord populations, respectively. To determine whether CSF-cNs belong to the V2b lineage, we analyzed whether specification of both groups of Gata2/3-expressing neurons are controlled by common mechanisms.

Previous studies have demonstrated that the transcription factor Foxn4, acting in p2 precursors, plays a pivotal role in cell fate decisions that regulate the production of inhibitory V2b neurons (Li et al., 2005; Peng et al., 2007; Del Barrio et al., 2007; Panayi et al., 2010). In E13.5 *Foxn4*-deficient spinal cords, the number of Chx10$^+$ V2a interneurons is expanded at the expense of V2b

Development (2016) 143, 880-891 doi:10.1242/dev.129254

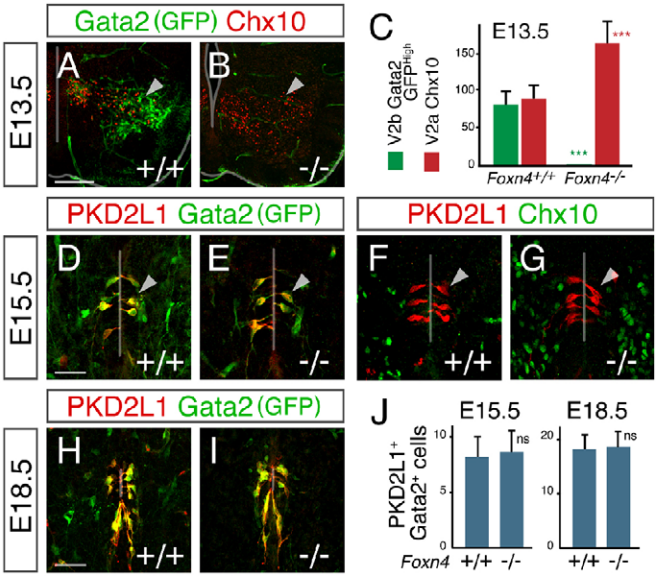

Fig. 4. Foxn4 controls early-born Gata2^{+} V2b neurons but is dispensable for Gata2^{+} CSF-cNs specification. (A-C) *Foxn4* mutants lack Gata2^{+} V2 interneurons. E13.5 spinal cords from wild-type and *Foxn4*$^{-/-}$ embryos stained for GFP (*Gata2*^{GFP}) and Chx10. The number of V2 neurons per section was quantified. V2b interneurons were identified by high levels of GFP (see Fig. S1O-T). Arrowheads indicate V2 neurons in the ventrolateral spinal cord. (D-J) E15.5 and E18.5 control or *Foxn4*$^{-/-}$ spinal cord sections stained for Pkd2l1, GFP (*Gata2*^{GFP}) and Chx10. CSF-cNs (Gata2^{+}Pkd2l1^{+}, arrowheads) develop normally in *Foxn4* mutants, contrasting with the absence of early-born Gata2^{+} neurons (B). (J) Number of Gata2^{+}Pkd2l1^{+} cells per section. Bars are mean±s.d.; ***P<0.001; ns, non-significant (Mann–Whitney test). Scale bars: 100 µm in A,B; 30 µm in D-G; 50 µm in H,I. Gray line indicates the ventricle.

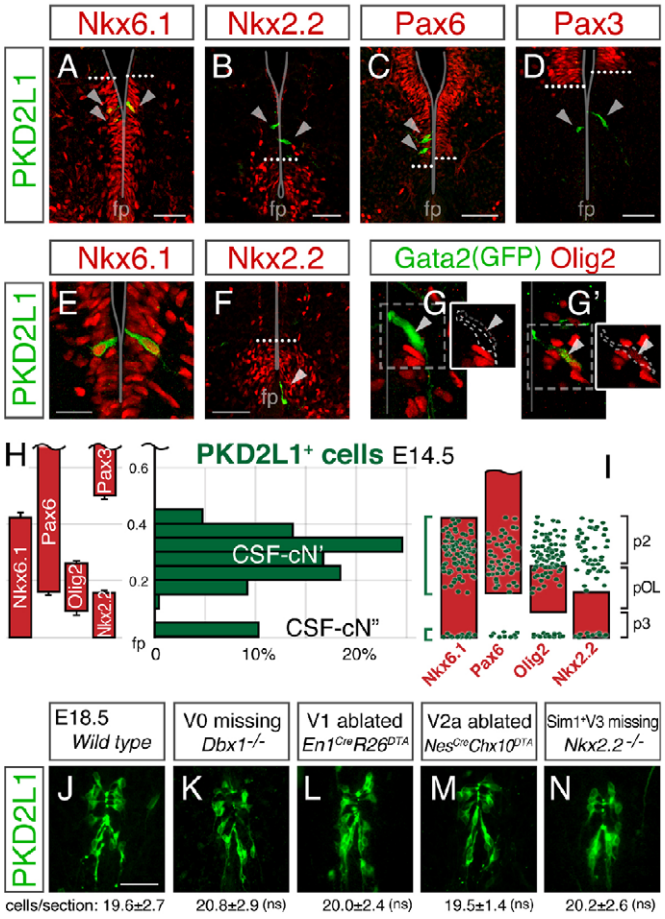

Fig. 5. CSF-cNs derive from ventral spinal cord progenitors. (A-F) E14.5 spinal cord sections stained for Pkd2l1 and Nkx6-1, Nkx2-2, Pax6 or Pax3. Few Pkd2l1^{+} cells are found at E14.5 (arrowheads). Most newly born Pkd2l1^{+} cells are positioned in territories that express Nkx6-1 and Pax6, and are named CSF-cN′. A second subset, termed CSF-cN″, is found at the boundary between the floor plate (fp) and the ventral Nkx2-2^{+} neuroepithelium (F, arrowhead). Dotted white line indicates the limit of each marker; gray line indicates the ventricle. (G) CSF-cNs′, identified by *Gata2*^{GFP}, negative for Olig2 (G, arrowheads), embedded in the p2 domain. (G′) A GFP^{+}CSF-cN′ expressing Olig2 (arrowheads; immersed in the pOL). At E14.5, 15% of GFP^{+}CSF-cN′ cells were Olig2^{+}. (H) Histogram of the dorsoventral position of 222 Pkd2l1^{+} cells at E14.5 (17 embryos): 90% are in the Pax6^{+}Nkx6.1^{+} area (64% in p2 domain, 26% in Olig2^{+} region) and 10% are positioned adjacent to the fp. The position of cells (green bars) and ventricular markers (red bars) are relative to the aperture of the ventricle. Bars are mean±s.d. (I) Position of CSF-cNs (green dots) analyzed together with Nkx6-1 (105 cells), Pax6 (n=60), Olig2 (n=98) or Nkx2-2 (n=57) staining, indicate that CSF-cN′ cells originate from the late p2 domain and the dorsal half of pOL, whereas CSF-cN″ cells are produced from progenitors adjacent to the floor plate. CSF-cNs were identified by Pkd2l1 or GFP in *Gata2*^{GFP} embryos. (J-N) CSF-cNs in E18.5 spinal cords lacking ventral neurons. Pkd2l1 immunohistochemistry on sections from wild type, *Dbx1*$^{lacZ/lacZ}$, *En1*^{Cre};*R26*^{DTA}, *Nestin:Cre;Chx10*^{DTA} and *Nkx2-2*$^{-/-}$. Mean±s.d.; ns, non-significant (Kruskal–Wallis test). Scale bars: 40 µm in A-D,F,J-N; 20 µm in E. See also Fig. S4.

neurons (Fig. 4A-C) identified by high levels of GFP in *Gata2*^{GFP} (Fig. S1O-T).

However, at E15.5, we identified Gata2^{+} cells by the ventricular surface in *Foxn4* mutants (Fig. 4D,E, arrowheads; *Gata2*^{GFP}), which co-express Pkd2l1 and are negative for Chx10 (Fig. 4D-G). This observation indicates that Gata2^{+} central canal neurons differentiate normally in the *Foxn4* mutants, contrasting with the complete absence of Gata2^{+} V2b cells in the lateral spinal cord (Fig. 4A-E). Furthermore, the number, location and morphology of Pkd2l1^{+}Gata2^{+} cells in *Foxn4* mutants at E18.5 were indistinguishable from those in wild-type embryos (Fig. 4H-J).

These experiments show that Gata2^{+}Pkd2l1^{+} cells do develop in the absence of *Foxn4*, and that the differentiation of V2b interneurons (early-born) and CSF-cNs (late-born) are governed by distinct genetic mechanisms. Together with our birthdate studies, these results demonstrate that CSF-cNs are indeed a cell population distinct from the previously described spinal Gata2/3^{+} V2b neurons.

CSF-cNs derive from late ventral spinal cord progenitors

To determine the dorsoventral origin of CSF-cNs, newly born Pkd2l1-expressing cells were mapped along the E14.5 neural tube in relation to the territories marked by Pax3, Nkx6-1, Pax6, Nkx2-2 and Olig2 (Fig. 5A-I) (Briscoe et al., 2000; Jessell, 2000; Briscoe and Novitch, 2008). As at E14.5 CSF-cNs have just become postmitotic and they do not lose their apical contact with the ventricular surface, this analysis reliably reflects their dorsoventral origin.

Pkd2l1^{+} cells were excluded from the Pax3^{+} dorsal zone (Fig. 5D,H). Most CSF-cNs (~90% at E14.5) arise from ventricular domains expressing Nkx6-1 and Pax6 (Fig. 5A-C,E,H,I). This pattern indicates that the major source of CSF-cNs are progenitors from the late p2 and pOL domains (Fig. 5H,I). Accordingly, a deeper inspection showed that 70% of these CSF-cNs are located dorsal to Olig2^{+} ventricular cells, whereas 30% of them are embedded in the dorsal half of the Olig2^{+} pOL domain (Fig. 5G,I). Thus, 90% of all

Development (2016) 143, 880-891 doi:10.1242/dev.129254

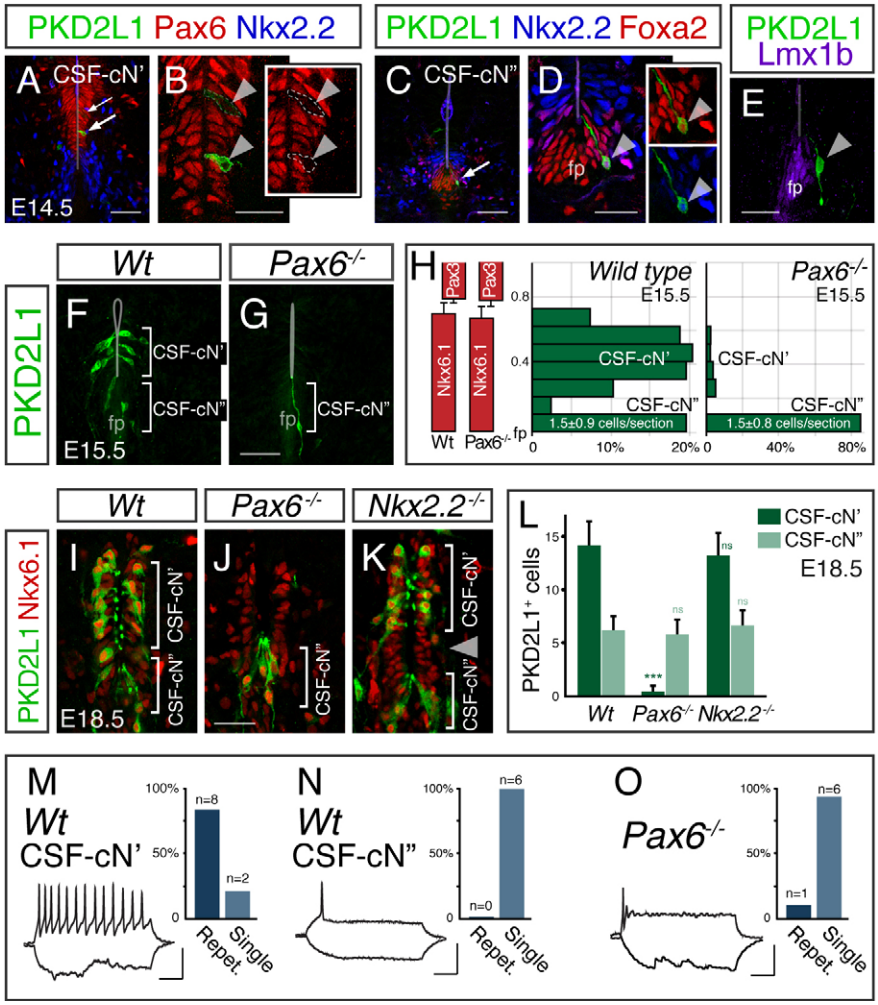

Fig. 6. Two subgroups of CSF-cNs originate from distinct progenitor pools. (A,B) E14.5 spinal cord showing newborn Pkd2l1$^+$ cells in Pax6-expressing territories. Arrows and arrowheads indicate Pkd2l1$^+$ neurons. (C-E) CSF-cN″, the ventral group of Pkd2l1$^+$ cells, originate close to the floor plate (fp; arrow in C; E14.5). CSF-cN″ cells express Nkx2-2 and Foxa2 (arrowheads in D) and are excluded from the fp, delineated by Lmx1b (E). (F-H) The development of CSF-cN′ cells requires Pax6. Immunohistochemistry for Pkd2l1 in E15.5 wild type and *Pax6* mutants. Histogram of the dorsoventral position of Pkd2l1$^+$ cells (Wt: *n*=237, *Pax6*$^{-/-}$: *n*=78) at E15.5. The distribution in Wt embryos reflects the two sources of Pkd2l1$^+$ cells: Nkx6.1$^+$Pax6$^+$ domain (F; ~80%; see also Fig. S4) and the boundary of the p3 domain with the floor plate. In *Pax6* mutants, CSF-cNs arise exclusively adjacent to the fp (G; ~85%). The number of CSF-cN″ cells were: Wt 1.5±0.9 and *Pax6*$^{-/-}$ 1.5±0.8 per section (not significant). (I-K) Immunostainings against Pkd2l1 and Nkx6-1 in E18.5 wild type, *Pax6* mutant and *Nkx2-2*$^{-/-}$. CSF-cN development is drastically altered in the *Pax6* null embryos, but unchanged in *Nkx2-2* mutants: Wt 20.6±2.7; *Pax6*$^{-/-}$ 6.5±1.4, (*P*<0.001); *Nkx2-2*$^{-/-}$ 20.6 ±3.1 cells per section (not significant). Arrowhead in K indicates the separation between the CSF-cN′ and CSF-cN″ subgroups in *Nkx2-2* mutants. (L) Quantification of Pkd2l1$^+$ cells lateral (CSF-cN′) and ventral (CSF-cN″) to the central canal shows that CSF-cN′ Pkd2l1$^+$ neurons are severely affected in *Pax6* mutants (***P<0.001 versus Wt), whereas the CSF-cN″ population remains unaltered. Bars are mean±s.d.; ns, non-significant difference; Kruskal–Wallis with post-hoc Dunn's test. (M-O) Electrophysiology of CSF-cNs identified by *Gata2*^{GFP} in E18.5 wild type and *Pax6* mutants. Graphs show the proportion of neurons eliciting repetitive or single action potentials in response to current injection (10 pA). Repetitive firing was found in 8/10 CSF-cN′ cells in Wt (M), whereas CSF-cN″ cells in Wt fired only once (*n*=6/6; N). The distribution of repetitive/single spiking in *Pax6*$^{-/-}$ versus Wt CSF-cN″ cells was non-significant, whereas the spiking pattern of *Pax6*$^{-/-}$ versus Wt CSF-cN′ cells was significantly different (*P*<0.05, Fisher's exact test). Representative recordings elicited by depolarizing/hyperpolarizing steps (0.5 s, 10pA) in Wt and in *Pax6*$^{-/-}$ slices are shown (trace scale bars: 50 mV, 100 ms). Scale bars: 40 µm in A,C,F,G; 20 µm in B,D,E; 30 µm in I-K. See also Fig. S5. Gray line indicates the ventricle.

CSF-cNs descend from progenitors in the p2 and dorsal half of the pOL domains.

Interestingly, our positional analysis revealed that a subgroup of CSF-cNs (~10% at E14.5) originate at the ventral pole of the neural tube, in the boundary between the Nkx2-2$^+$ neuroepithelium and the floor plate (Fig. 5F, arrowhead; Fig. 5H,I). Positional mappings at E15.5 yielded a similar distribution (Fig. S4).

Further evidence that CSF-cNs do not belong to V0, V1, V2a and Sim1$^+$ V3 populations, comes from animals lacking these cell types (Fig. 5J-N). The number of Pkd2l1-expressing cells was found to be unaltered in *Dbx1*$^{-/-}$, *En1*^{Cre}*;R26*^{DTA}, *Nestin:Cre;Chx10*^{DTA} and *Nkx2-2*$^{-/-}$ E18.5 embryos (Pierani et al., 2001; Lanuza et al., 2004; Gosgnach et al., 2006; Crone et al., 2008; Briscoe et al., 1999).

Two subsets of CSF-cNs originate from distinct progenitor pools

Our analysis indicates that CSF-cNs derive from two distinct sources in the germinative zone, with most Pkd2l1$^+$ neurons produced from Nkx6-1$^+$Pax6$^+$ territories and a smaller proportion from Pax6-negative precursors by the floor plate (Fig. 5A-I; Fig. S4). We named these embryonic subgroups CSF-cN′ and CSF-cN″, respectively (Fig. 5H), consistent with zebrafish Kolmer–

Development (2016) 143, 880-891 doi:10.1242/dev.129254

Agduhr cells (Park et al., 2004). When inspecting these two subsets, we found that although the most dorsal subgroup of Pkd2l1$^+$ cells (CSF-cN′) locate within the Pax6-expressing ventricular zone (Fig. 6A,B; Fig. S5A), this transcription factor is sharply downregulated during CSF-cN neurogenesis (Fig. 6A,B). Accordingly, in cells that have not yet reached high levels of Pkd2l1, low levels of Pax6 can still be detected (Fig. 6B, upper arrowhead), indicating that CSF-cN′ cells are descendants of Pax6 precursors of the p2 and dorsal part of the pOL domain.

To define whether Pkd2l1$^+$ cells by the floor plate (CSF-cN″) come from a different progenitor pool, we analyzed the presence of the p3 marker Nkx2-2 and of Foxa2, which is expressed in the floor plate and the ventral-third of p3 cells (Fig. 6C,D). We found that CSF-cN″ cells are positive for Nkx2-2 and Foxa2 (Fig. 6D; 90 and 92%, respectively), but do not express Lmx1b, a marker of the non-neurogenic floor plate (Fig. 6E), or Pax6 (Fig. S5B). These results indicate that ventral Pkd2l1$^+$ neurons derive from Nkx2-2$^+$ precursors in the proximity of the floor plate.

To understand CSF-cN development better, we evaluated whether Pax6 is required for their specification, and if its absence preferentially affects any of their subsets. First, we analyzed CSF-cNs in E15.5 *Pax6*$^{-/-}$ embryos and found that the number of Pkd2l1-expressing cells is drastically diminished [Fig. 6F,G; wild type (Wt):6.9±1.7; *Pax6*$^{-/-}$:1.6±0.8 cells/section; $P<0.001$]. Remarkably, in *Pax6* mutant spinal cord, Pkd2l1$^+$ cells at the boundary between the p3 ventricular zone and the floor plate (CSF-cN″) remain unaltered (Fig. 6G,H), whereas those that originate more dorsally (CSF-cN′) are missing. In *Pax6* mutants, the CSF-cN″ subset represents ∼85% of the remaining Pkd2l1$^+$ cells (Fig. 6H), whereas in their wild-type littermates it accounts for 15-20% at E15.5 (Fig. 6H; Fig. S4H).

Our results show that CSF-cNs originate from two different regions of the ventricular zone and that Pax6 is exclusively required for the production of CSF-cNs from progenitors in the p2-pOL domain. We tested next the hypothesis that the postnatal organization of CSF-cNs either lateral or ventral to the central canal (see above; Fig. 1J-K′) reflects these ontogenetic differences. By examining the *Pax6*$^{-/-}$ spinal cord at E18.5, we found a marked reduction in the number of Pkd2l1$^+$ cells (Fig. 6I,J,L). CSF-cNs remaining in *Pax6* mutants were exclusively located ventral to the central canal, whereas CSF-cNs settling laterally were absent (Fig. 6J,L). This finding was further confirmed by assessing Gata2 expression by *in situ* hybridization (Fig. S5F,G). The correlation found in E15.5 and E18.5 *Pax6* mutants indicates that CSF-cN′ and CSF-cN″ populations contribute to anatomically distinct subsets of CSF-cNs in the postnatal spinal cord.

Although Nkx2-2 is expressed in CSF-cNs at the p3-floor plate boundary, we found that it is dispensable for the production of CSF-cN″ cells, as no differences were found in their number in *Nkx2-2* mutants (Fig. 6K,L). Nonetheless, it is interesting that E18.5 *Nkx2-2*$^{-/-}$ spinal cord, in which the lumen fails to properly close ventrally, shows a broader separation between CSF-cN″ and CSF-cN′ cells (Fig. 6K, arrowhead), supporting the idea that they constitute two different CSF-cN subgroups.

To understand further the differences between these two CSF-cN subpopulations, we evaluated the electrophysiological properties of CSF-cN′ and CSF-cN″ cells, and compared them with CSF-cNs in *Pax6*-null spinal cords (Fig. 6M-O). In *Gata2*^{GFP} animals, repetitive spiking was observed in 80% of GFP$^+$CSF-cNs′ (Fig. 6M; n=8/10) but in none of the CSF-cN″ cells, which fired only once (Fig. 6N; n=0/6). When this analysis was performed in *Pax6* mutants, most CSF-cNs produced a single spike (Fig. 6O; n=6/7), resembling the CSF-cN″ subset in wild-type embryos. These experiments show that CSF-cN′ and CSF-cN″ cells exhibit different electrophysiological properties, and that neurons developing in *Pax6*-null spinal cord display functional properties of CSF-cN″ cells. These results fully confirm that CSF-cN″ cells, which originate from the most ventral precursors, are those Pkd2l1$^+$ neurons ventral to the central canal in the postnatal spinal cord.

In summary, differences found in ontogeny, location and physiological properties indicate the existence of two distinct groups of CSF-cNs: those settled within the lateral wall of the central canal, born from late p2/pOL cells (CSF-cN′), and those positioned in the ventral pole of the central canal that originate from precursors bordering the floor plate (CSF-cN″).

DISCUSSION

This study demonstrates that CSF-cNs are produced in the mouse ventral spinal cord during advanced embryonic stages, previously thought to generate only glial cells and ependymocytes. We show that CSF-cNs comprise a late-born population of Gata2/3-expressing cells different from early-born V2b interneurons. Gata2/3$^+$ neurons of the central canal are identified by unique morphological features and the selective expression of Pkd2l1 and Pkd1l2. Furthermore, we show that mouse CSF-cNs can be subdivided into two distinct subgroups that develop from separate progenitor domains and are located at different positions around the postnatal central canal.

CSF-cNs are late-born Gata2/3$^+$ neurons

Ependymal cells lining the central canal of the spinal cord are derived from ventral neuroepithelial progenitors (Fu et al., 2003; Yu et al., 2013). The ependyma is composed of a layer of ciliated mural ependymocytes interspersed with tanycytes and CSF-contacting neurons (Bruni, 1998; Meletis et al., 2008; Sabourin et al., 2009; Marichal et al., 2012). Our genetic-tracing experiments with *Gata3*^{Cre} and *Gata2*^{GFP} selectively identified spinal CSF-cNs, which exhibit a unique morphology with a prominent dendritic process through the ependymal layer (Vigh and Vigh-Teichmann, 1971, 1998; Vigh et al., 1983) and express Pkd2l1 (Huang et al., 2006; Orts-Del'Immagine et al., 2014, 2016; Djenoune et al., 2014).

The transcription factors Gata2 and Gata3 have been considered to be selective indicators of spinal V2b identity (Karunaratne et al., 2002; Peng et al., 2007; Lundfald et al., 2007; Zhang et al., 2014). However, we provide compelling evidence that CSF-cNs do not belong to the V2b neuronal lineage, although both populations share the expression of Gata2/3 proteins. Contrasting with the mandatory activity of Foxn4 for V2b neuron specification (Li et al., 2005; Peng et al., 2007; Del Barrio et al., 2007), we found that CSF-cNs develop normally in the *Foxn4* mutant spinal cord. Furthermore, our expression analysis of Gata2 and Pkd2l1, in conjunction with birthdating results, reveals strict timing differences in the generation of Gata2/3$^+$ spinal populations. Therefore, CSF-cNs are a novel population of late-born Gata2/3$^+$ neurons differentiation of which is controlled by genetic mechanisms distinct from those that specify early-born Gata2/3$^+$ V2b interneurons (Fig. 7).

In addition, our results exclude the possibility that CSF-cNs are related to other V2 cell types described so far. Pkd2l1$^+$ cells do not express the V2a marker Chx10, nor persist after V2a ablation in *Chx10*^{DTA} mice; they do not maintain Pax6 expression, characteristic of a subset of V2b cells (Panayiotou et al., 2013); and, unlike V2b and V2c, CSF-cN development is not dependent on Foxn4 (Li et al., 2005; Peng et al., 2007; Del Barrio et al., 2007;

Development (2016) 143, 880-891 doi:10.1242/dev.129254

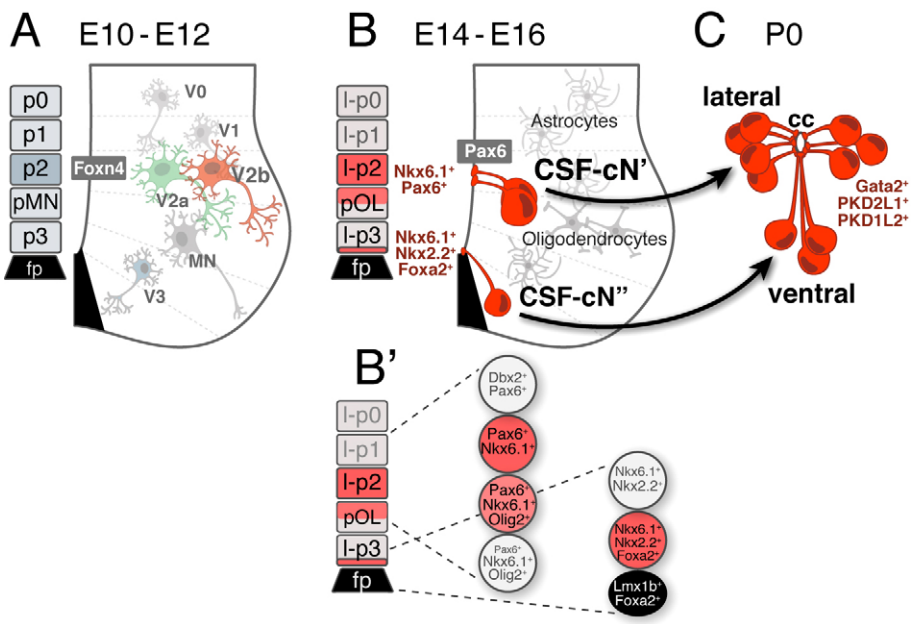

Fig. 7. Summary of the development of spinal CSF-cNs. (A) Schematic of E10-E12 ventral spinal cord showing progenitor domains and early-born neurons. Defined domains of progenitors in the dorsoventral axis of the neural tube give rise to motoneurons (MN) and V0-V3 interneurons. The transcription factor Foxn4, expressed in p2 progenitors, is essential for the specification of early-born Gata2$^+$Gata3$^+$ V2b interneurons. (B,B′) Schematic of E14-E16 ventral spinal cord showing differentiation of Gata2$^+$Gata3$^+$ CSF-cNs along with astrocytes and oligodendrocyte progenitor cells. CSF-cN′ cells are born from late Nkx6-1$^+$Pax6$^+$ progenitors in the p2 and the dorsal half of the pOL domains. CSF-cN″ cells arise from Nkx2-2$^+$Foxa2$^+$ p3 cells in the frontier with the floor plate (fp). The transcription factor Pax6 selectively controls the development of the CSF-cN′ subset. B′ shows the transcription factor identity of CSF-cN progenitors. (C) In the postnatal spinal cord, CSF-cN′ and CSF-cN″ cells are organized lateral and ventral to the central canal (cc), respectively.

Panayi et al., 2010). Furthermore, we show that CSF-cNs differentiate several days after V2a-d neurons have developed.

Importantly, our experiments demonstrate that CSF-cNs are produced at unusually late stages, when spinal cord neurogenesis is essentially extinguished and ventricular precursors are broadly committed towards glial and ependymal fates (Rowitch and Kriegstein, 2010; Altman and Bayer, 1984; Rowitch, 2004). BrdU labeling shows that CSF-cN progenitors still divide at ∼E13.5-E14.5, 24-48 h before the initiation of Gata2 and Pkd2l1 expression upon their postmitotic conversion. These results are consistent with our analysis of Pkd2l1 in the embryonic chick spinal cord and recent observations of CSF-cNs in developing rodents (Kútna et al., 2014; Djenoune et al., 2014). We propose that late birthdate is a characteristic of central canal neurons in amniotes, in contrast to CSF-cNs in fish and amphibians (see below). Additionally, the developmental origin of CSF-cNs indicates that they are born intermingled with oligodendrocytes and vA2 and vA3 astrocytes (Hochstim et al., 2008; Tsai et al., 2012; Rowitch and Kriegstein, 2010; Zhou and Anderson, 2002; Lu et al., 2002). In the future, it will be important to determine the mechanism that suppresses glial and ependymal fate in late progenitors of the ventral spinal cord to instruct the production of central canal neurons.

These results highlight the importance of the timing of neurogenesis in neuronal diversification. Although other cases have been reported in which the temporal component contributes to neuronal diversity in the spinal cord (Gross et al., 2002; Stam et al., 2012), we provide robust evidence of neuronal differentiation occurring in what has been classically termed the gliogenic phase, proving that neurogenic potential is retained in the late ventricular zone progenitors.

The double developmental origin of CSF-cNs

In the mouse spinal cord, the majority of CSF-cNs, here termed the CSF-cN′ population, are produced from progenitors belonging to the late p2 and the dorsal half of pOL domains. A smaller proportion of Pkd2l1$^+$ neurons (CSF-cN″) are born from p3 cells bordering the floor plate (Fig. 7B).

We show that, in the mouse, CSF-cN′ cells derive from Nkx6-1$^+$Pax6$^+$ progenitors and that Pax6 selectively controls their development. In our work, three lines of evidence suggest that the lack of CSF-cN′ cells in *Pax6* mutants is not attributed to the early actions of this transcription factor in dorsoventral cell identity (Ericson et al., 1997; Briscoe et al., 1999). First, the extent of Nkx6-1 is not modified in *Pax6*$^{-/-}$ spinal cord. Second, the differentiation of V2a/b neurons, which precedes CSF-cN′ development, is not affected by Pax6 absence (Fig. S5C-E; Zhang et al., 2014). Third, *Pax6;Nkx2-2* double mutation did not rescue CSF-cN′ development (not shown). This argues that, similar to V1 specification, the expansion of Nkx2-2, normally repressed by Pax6 (Ericson et al., 1997; Briscoe et al., 1999), is not responsible for the lack of the CSF-cN′ population in *Pax6* mutants. Altogether, these results suggest that Pax6 controls CSF-cN development by acting in late progenitors that give rise to CSF-cN′.

In common with CSF-cNs in the mouse, Kolmer–Agduhr (KA) cells in the zebrafish neural tube have a dual progenitor source and are composed of two subsets, KA′ and KA″ (Park et al., 2004; Shin et al., 2007; Schäfer et al., 2007; Yang et al., 2010; Huang et al., 2012; Djenoune et al., 2014). Mouse CSF-cN′ cells display similarities with zebrafish KA′ cells, as both are produced at rather similar dorsoventral spinal cord locations. Mapping experiments using transgenic *olig2*:EGFP zebrafish have shown that all KA′ cells derive from the pMN domain together with motoneurons (Park et al., 2004; Shin et al., 2007; Yang et al., 2010; Djenoune et al., 2014). By contrast, in the mouse, we found that CSF-cN′ cells are mostly produced from progenitors with p2 identity (∼70%) with only ∼30% originated from the Olig2$^+$ domain. It is possible that this difference between mouse CSF-cN′ and zebrafish KA′ cells is a consequence of their timing of neurogenesis (see below). In the mouse, Olig2 is transiently present in early p2 progenitors, dorsally to its normal expression domain (Chen et al., 2011; Dessaud et al., 2010), but CSF-cNs only begin to appear several days later. It remains to be determined whether Olig2 plays any role in the development of CSF-cN′ cells in the mouse.

Our experiments have also determined that progenitor cells at the frontier with the floor plate are a second source of CSF-cNs. The expression of Nkx2-2 and Foxa2, but not Lmx1b, indicate that CSF-cN″ cells derive from the ventral-most p3 domain bordering the floor plate. We propose that CSF-cN″ cells are homologous to KA″

Development (2016) 143, 880-891 doi:10.1242/dev.129254

cells in zebrafish spinal cord, which similarly express *nkx2.2* genes and are born from neuroepithelial cells lateral to the floor plate (Schäfer et al., 2007; Strähle et al., 2004; Yang et al., 2010). Although CSF-cN″ cells are Nkx2-2 positive, they develop normally in *Nkx2-2*-deficient embryos. Given that Nkx2-9 transiently overlaps with Nkx2-2 in the most ventral p3 cells of the mouse neural tube (Briscoe et al., 1999; Holz et al., 2010) and zebrafish KA″ are only completely lost after *nkx2.2a/b;nkx2.9* knockdown (Yang et al., 2010), it is likely that in the absence of Nkx2-2, CSF-cN″ cells rely on Nkx2-9 for their specification. The analysis of the CSF-cN″ population in *Nkx2-2;Nkx2-9* mutants will elucidate the role of Nkx2 transcription factors in its ontogeny.

The dual developmental origin of CSF-cNs is reminiscent of the multiple sources of oligodendrocytes in the spinal cord and Cajal–Retzius cells in the telencephalon (Vallstedt et al., 2005; Bielle et al., 2005). Similarly, it is likely that, although being distinct subpopulations, CSF-cN′ and CSF-cN″ partially share the specification program that determines their phenotypic characteristics, downstream of different initial determinants.

Heterochronic development of CSF-cNs in vertebrates

CSF-cNs in mouse and KA cells in zebrafish display similarities in their dorsoventral positioning, as well as in their marker expression, but they exhibit striking differences in development timing. In this study, we demonstrate that in the mouse and chick spinal cord, CSF-cNs are produced during advanced embryonic stages, after the neurogenic period. By contrast, KA cells in zebrafish and amphibians are born exclusively during early phases of spinal cord development (Dale et al., 1987a; Shin et al., 2007).

This heterochrony can be established by comparing the timing of CSF-cN or KA differentiation with the birth of motoneurons, interneurons and oligodendrocytes. In zebrafish, KA′ cells are born along with primary motoneurons between 10 and 15 h post-fertilization (hpf) (Park et al., 2004; Shin et al., 2007), whereas KA″ cells arise from early ventral precursors in their last division at ∼10 hpf (Yeo and Chitnis, 2007; Huang et al., 2012; Shin et al., 2007). In the mouse, the production of motoneurons and ventral interneurons precedes CSF-cN differentiation by more than 2 days. Conversely, zebrafish VeLD and CiD interneurons, the homologs of mouse V2b and V2a neurons, appear at about 17 hpf, when KA cells have already been born (Kimura et al., 2008; Batista et al., 2008; Shin et al., 2007). More ventrally, *sim1*-expressing V3 neurons are seen at ∼30 hpf, when KA″ have fully differentiated (Schäfer et al., 2007; Yang et al., 2010). The third parameter to date differences is the presence of glial cells. As discussed above, mouse CSF-cNs are generated during the developmental phase that produces astrocytes and oligodendrocytes. By contrast, the generation of zebrafish KA cells clearly precedes oligodendrocyte precursor specification, which begins at ∼36 hpf (Kirby et al., 2006).

Thus, although in the mouse and chick spinal cord CSF-cNs arise from seemingly unique late neurogenic events, the differentiation of KA cells in zebrafish and *Xenopus* takes place before or at the same time as that of other ventral spinal neurons. The contrast in relative timings can be attributed to pre- or post-displacements (Smith, 2003; McKinney and McNamara, 1991) and can bring about differential evolutionary adaptations to specific selection pressures. This heterochronic sequence might be related to the different functions of CSF-cNs and KA cells in amniotes and non-amniotes, respectively, such as the essential role of KA cells in larval swimming (Wyart et al., 2009; Fidelin et al., 2015), or to constraints, such as the requirement to produce larger cohorts of early-born ventral neurons in walking vertebrates. A more comprehensive comparative analysis of the ontogeny of CSF-cNs in vertebrates will be important to define the polarity of the change in phylogeny, and how this shift in developmental timing relates to adaptive changes or constraints.

On the physiological properties and the role of CSF-cNs

CSF-cNs have been found in every vertebrate species examined so far, from lamprey to primates (Vigh and Vigh-Teichmann, 1971; Vigh et al., 1977, 1983; Barber et al., 1982; Dale et al., 1987b; Stoeckel et al., 2003; Jalalvand et al., 2014; Djenoune et al., 2014; Reali et al., 2011). However, despite this evolutionary conservation, their function has not yet been fully elucidated. Gata2^{+} neurons of the central canal in newborn and young mice exhibit molecular and physiological characteristics of immature neurons, in agreement with previous observations (Stoeckel et al., 2003; Marichal et al., 2009; Sabourin et al., 2009; Orts-Del'Immagine et al., 2014, 2012; Kútna et al., 2014).

The strategic location of CSF-cNs in the interface between the CSF and the spinal cord parenchyma has generated much speculation about their functions (Vigh et al., 2004; Vigh and Vigh-Teichmann, 1998). It has been suggested that CSF-cNs might act as mechano- or chemosensory neurons intrinsic to the central nervous system that detect either CSF movement within the central canal or variations in its composition, most notably its pH (Orts Del'Immagine et al., 2016, 2012; Huang et al., 2006; Wyart et al., 2009). A recent study has shown the importance of the Pkd2l1 channel in CSF-cNs; Pkd2l1 is able to generate depolarizations large enough to trigger action potentials and thus act as a spike generator (Orts Del'Immagine et al., 2016). Our identification that Pkd1l2 is selectively co-expressed with Pkd2l1 suggests that Pkd1l2 might regulate Pkd2l1 activity and/or its targeting to the membrane to avoid an overexcitation of CSF-cNs (Orts Del'Immagine et al., 2016; Ishimaru et al., 2006; Semmo et al., 2014; DeCaen et al., 2013).

In view of the dual developmental origin of CSF-cNs in the embryonic spinal cord, the differences found in their physiological properties and the strict correspondence with their location in the postnatal central canal, it is tempting to speculate that each CSF-cN subgroup might have specific and dissimilar physiological functions.

MATERIALS AND METHODS

Animals

Experiments were conducted according to protocols approved by the Institutional Animal Care and Use Committee of Instituto Leloir. Genotyping of *Gata3*^{Cre} (Zhang et al., 2014), *Gata2*^{GFP} (Suzuki et al., 2006) and *Gata3*^{lacZ} (van Doorninck et al., 1999) (obtained from Doug Engel, University of Michigan, MI, USA), *Foxn4*^{lacZ} (kindly provided by Mengqing Xiang, University of Medicine and Dentistry of New Jersey, NJ, USA) (Li et al., 2004), *Pax6-Small eye*, *Nkx2-2* (Briscoe et al., 1999), *Sim1*^{Cre} (Zhang et al., 2008), *En1*^{Cre} (Sapir et al., 2004), *Dbx1*^{lacZ} (Pierani et al., 2001), *Nestin:Cre*,*Chx10*^{DTA} (Crone et al., 2008) (embryos kindly provided by Kamal Sharma, University of Illinois-Chicago, IL, USA), *R26*^{DTA} (Brockschnieder et al., 2004), *Gad1*^{GFP} (Tamamaki et al., 2003), *Sst*^{Cre} (Taniguchi et al., 2011), and the conditional reporters *R26*^{GFP} (Mao et al., 2001), *ZnG* (Zhang et al., 2008) and *Ai14 td-Tomato* (Madisen et al., 2010) mice was performed by PCR.

For bromodeoxyuridine labeling, females were injected intraperitoneally with BrdU (35 or 50 mg/kg body weight) for multiple or single administrations, respectively. Tissue was fixed in 4% paraformaldehyde (PFA), equilibrated in 20% sucrose prior to embedding (Cryoplast, Biopack) and cryosectioned (Leica CM1850 cryostat; 30 µm).

Development (2016) 143, 880-891 doi:10.1242/dev.129254

Immunohistochemistry and *in situ* hybridization

For immunohistochemistry, sections were treated with blocking solution (5% HI-serum, 0.1% TritonX-100 in PBS) for 1 h and primary antibodies in blocking were incubated overnight at 4°C (Carcagno et al., 2014). Antibodies used were: anti-Nkx2-2 [74.5A5, Developmental Studies Hybridoma Bank (DSHB), University of Iowa, USA; 1:20], anti-Nkx6-1 (F55A10, DSHB; 1:20), anti-Pax6 (cat. #pax6, DSHB; 1:20), anti-Pkd2l1 (from Charles Zuker, Columbia University, NY, USA; 1:5000), anti-GFP (GFP1020, Aves Labs; 1:1000), anti-Gata2 (from Kamal Sharma, University of Illinois at Chicago, IL, USA; 1:1000), anti-Chx10 (from Sam Pfaff, Salk Institute, CA, USA; 1:1000), anti-Sox2 (SC17320, Santa Cruz Biotechnology; 1:300), anti-NeuN (A60, Chemicon; 1:500), anti-β-III tubulin (MMS435P, Covance; 1:500), anti-Gfap (from Fred Gage, Salk Institute, CA, USA; 1:2500), anti-vimentin (AB5733, Chemicon; 1:1000), anti-β-gal (from Martyn Goulding, Salk Institute; 1:1000), anti-BrdU (MCA2060T, ImmunoDirect; 1:250), anti-dsRed (632496, Clontech; 1:300) and anti-Olig2 (AB9610, Chemicon; 1:1000). Rat anti-chick Pkd2l1 antibody was generated using *Brucella* lumazine synthase (BLS) as peptide carrier (Laplagne et al., 2004). For detection, Cy-labeled species-specific secondary antibodies (Jackson ImmunoResearch) were incubated for 3 h at room temperature. Sections were mounted with PVA-DABCO or dehydrated in ethanol/xylene series and mounted with DPX.

Non-radioactive *in situ* hybridizations were performed as described (Carcagno et al., 2014). Sections were fixed with 4% PFA and washed with PBS. Tissue was treated for 3 min with proteinase K (3 µg/ml), followed by 4% PFA for 10 min and PBS washes. Slides were incubated in triethanolamine-acetic anhydrate, pH 8.0, for 10 min and permeabilized with 1% TritonX-100 for 30 min. Sections were incubated for 2 h with hybridization solution (50% formamide, 5×SSC, 5×Denhardt's solution, 250 µg/ml yeast tRNA). Digoxigenin (DIG)-labeled RNA probes used were Pkd1l2 (5663-6470 of mouse *Pkd1l2* mRNA)and chick-Pkd2l1 (2479-2734 of chicken *Pkd2l1* mRNA predicted sequence), Gata2 (Carcagno et al., 2014), vGAT (Slc32a1) and vGluT2 (Slc17a6) (Lanuza et al., 2004), Gad1 and Gad2 (Cheng et al., 2004), vAChT (Slc18a3) (Carcagno et al., 2014). DIG-labeled probes were diluted in hybridization solution, denatured and incubated onto slides for 14 h at 68°C. Sections were washed three times, for 45 min at 68°C with 1×SSC, 50% formamide. For detection, slides were blocked in blocking solution with 10% HI-serum for 2 h and incubated overnight at 4°C with alkaline phosphatase-labeled anti-DIG antibody (11093274910, Roche; 1:2500). After washing, enzymatic activity was developed with BCIP and NBT in reaction solution (0.1 M Tris-HCl pH 9.5, 50 mM $MgCl_2$, 0.1 M NaCl, 0.1% Tween-20).

For immuno-*in situ* double staining, sections were incubated with antibodies after developing the DIG *in situ* reaction. For BrdU staining, acidic antigen retrieval was performed prior to immunodetection. Images were captured using Zeiss Axioplan microscope, Zeiss LSM5-Pascal and LSM510-Meta confocal microscopes and assembled using Adobe Photoshop and Illustrator software.

Acute spinal cord slice recordings

Recordings were performed as described (Gosgnach et al., 2006; Zhang et al., 2008). *Gata2*^{GFP} spinal cords were dissected in chilled low-calcium Ringer's solution and cut using a vibrating microtome (Leica VT1200S). Slices were transferred to a recording chamber on Olympus BX61WI microscope at room temperature. Recordings were obtained using Axopatch 200B amplifiers, and digitized using pClamp10 software (Molecular Devices). Capacitance and input resistance were obtained from currents evoked by a 10-mV hyperpolarizing step. Voltage-dependent currents were recorded by applying conditioning steps of 10 mV from −60 mV holding potential. Spiking responses were recorded by applying depolarizing current steps (10 pA, 500 ms) under current clamp, keeping the cells at −60 mV.

Quantification and statistical analysis

Cell counts were performed on a minimum of ten sections from at least three embryos. Non-parametric Mann–Whitney U test, Kruskal–Wallis one-way analysis of variance with post hoc Dunn's multiple comparison test or Fisher's exact test were performed (GraphPad Software). Results are shown as mean±s.d. unless otherwise specified and considered statistically significant when $P<0.05$.

Acknowledgements

We deeply thank Martyn Goulding (The Salk Institute) for generously sharing reagents and tissue, and providing insights that assisted the research. We thank Mengqing Xiang, Doug Engel, John Rubenstein, Tom Jessell and Kamal Sharma for mice or embryos; Charles Zuker, Kamal Sharma, Sam Pfaff, Quifu Ma and Fernando Pitossi for antibodies or probes; Fernando Goldbaum lab (Leloir Institute) for collaboration with the BLS-antigen expression system; and Susana Godoy (Tres Arroyos) for chicken eggs.

Competing interests

The authors declare no competing or financial interests.

Author contributions

Y.L.P. and M.M.S. performed most of the experiments and analyzed data; D.J.D.B., A.L.C. and G.M.L. performed additional experiments and analyzed results; A.M.-B. and A.F.S. contributed to electrophysiological analysis; G.M.L. designed the research; the manuscript was edited by all authors.

Funding

This work was supported by the Agencia Nacional de Promoción Científica y Tecnológica of Argentina [PICT2011-1350 and PRH-PICT09-116 to G.M.L.]; the International Brain Research Organization (IBRO, Return Home Award to G.M.L.); and the Fogarty International Center, National Institutes of Health [FIRCA-NIH 1 R03 TW008026 to G.M.L.]. G.M.L., A.M.-B., A.L.C. and A.F.S. are investigators of the Consejo Nacional de Investigaciones Científicas y Técnicas (CONICET). Y.L.P., M.M.S. and D.J.D.B. were sponsored by fellowships from CONICET. Deposited in PMC for release after 12 months.

Supplementary information

Supplementary information available online at
http://dev.biologists.org/lookup/suppl/doi:10.1242/dev.129254/-/DC1

References

Altman, J. and Bayer, S. A. (1984). The development of the rat spinal cord. *Adv. Anat. Embryol. Cell Biol.* **85**, 1-164.

Balaskas, N., Ribeiro, A., Panovska, J., Dessaud, E., Sasai, N., Page, K. M., Briscoe, J. and Ribes, V. (2012). Gene regulatory logic for reading the Sonic Hedgehog signaling gradient in the vertebrate neural tube. *Cell* **148**, 273-284.

Barber, R. P., Vaughn, J. E. and Roberts, E. (1982). The cytoarchitecture of GABAergic neurons in rat spinal cord. *Brain Res.* **238**, 305-328.

Batista, M. F., Jacobstein, J. and Lewis, K. E. (2008). Zebrafish V2 cells develop into excitatory CiD and Notch signalling dependent inhibitory VeLD interneurons. *Dev. Biol.* **322**, 263-275.

Bielle, F., Griveau, A., Narboux-Nême, N., Vigneau, S., Sigrist, M., Arber, S., Wassef, M. and Pierani, A. (2005). Multiple origins of Cajal-Retzius cells at the borders of the developing pallium. *Nat. Neurosci.* **8**, 1002-1012.

Briscoe, J. and Novitch, B. G. (2008). Regulatory pathways linking progenitor patterning, cell fates and neurogenesis in the ventral neural tube. *Philos. Trans. R. Soc. B Biol. Sci.* **363**, 57-70.

Briscoe, J., Sussel, L., Serup, P., Hartigan-O'Connor, D., Jessell, T. M., Rubenstein, J. L. and Ericson, J. (1999). Homeobox gene Nkx2.2 and specification of neuronal identity by graded Sonic hedgehog signalling. *Nature* **398**, 622-627.

Briscoe, J., Pierani, A., Jessell, T. M. and Ericson, J. (2000). A homeodomain protein code specifies progenitor cell identity and neuronal fate in the ventral neural tube. *Cell* **101**, 435-445.

Brockschnieder, D., Lappe-Siefke, C., Goebbels, S., Boesl, M. R., Nave, K.-A. and Riethmacher, D. (2004). Cell depletion due to diphtheria toxin fragment A after Cre-mediated recombination. *Mol. Cell. Biol.* **24**, 7636-7642.

Bruni, J. E. (1998). Ependymal development, proliferation, and functions: a review. *Microsc. Res. Tech.* **41**, 2-13.

Bylund, M., Andersson, E., Novitch, B. G. and Muhr, J. (2003). Vertebrate neurogenesis is counteracted by Sox1-3 activity. *Nat. Neurosci.* **6**, 1162-1168.

Carcagno, A. L., Di Bella, D. J., Goulding, M., Guillemot, F. and Lanuza, G. M. (2014). Neurogenin3 restricts serotonergic neuron differentiation to the hindbrain. *J. Neurosci.* **34**, 15223-15233.

Chen, J.-A., Huang, Y.-P., Mazzoni, E. O., Tan, G. C., Zavadil, J. and Wichterle, H. (2011). Mir-17-3p controls spinal neural progenitor patterning by regulating Olig2/Irx3 cross-repressive loop. *Neuron* **69**, 721-735.

Cheng, L., Arata, A., Mizuguchi, R., Qian, Y., Karunaratne, A., Gray, P. A., Arata, S., Shirasawa, S., Bouchard, M., Luo, P. et al. (2004). Tlx3 and Tlx1 are post-mitotic selector genes determining glutamatergic over GABAergic cell fates. *Nature Neurosci.* **7**, 510-517.

Development (2016) 143, 880-891 doi:10.1242/dev.129254

Crone, S. A., Quinlan, K. A., Zagoraiou, L., Droho, S., Restrepo, C. E., Lundfald, L., Endo, T., Setlak, J., Jessell, T. M., Kiehn, O. et al. (2008). Genetic ablation of V2a ipsilateral interneurons disrupts left-right locomotor coordination in mammalian spinal cord. *Neuron* **60**, 70-83.

Dale, N., Roberts, A., Ottersen, O. P. and Storm-Mathisen, J. (1987a). The development of a population of spinal cord neurons and their axonal projections revealed by GABA immunocytochemistry in frog embryos. *Proc. R. Soc. B Biol. Sci.* **232**, 205-215.

Dale, N., Roberts, A., Ottersen, O. P. and Storm-Mathisen, J. (1987b). The morphology and distribution of 'Kolmer-Agduhr cells', a class of cerebrospinal-fluid-contacting neurons revealed in the frog embryo spinal cord by GABA immunocytochemistry. *Proc. R. Soc. B Biol. Sci.* **232**, 193-203.

DeCaen, P. G., Delling, M., Vien, T. N. and Clapham, D. E. (2013). Direct recording and molecular identification of the calcium channel of primary cilia. *Nature* **504**, 315-318.

Del Barrio, M. G., Taveira-Marques, R., Muroyama, Y., Yuk, D.-I., Li, S., Wines-Samuelson, M., Shen, J., Smith, H. K., Xiang, M., Rowitch, D. et al. (2007). A regulatory network involving Foxn4, Mash1 and delta-like 4/Notch1 generates V2a and V2b spinal interneurons from a common progenitor pool. *Development* **134**, 3427-3436.

Dessaud, E., Ribes, V., Balaskas, N., Yang, L. L., Pierani, A., Kicheva, A., Novitch, B. G., Briscoe, J. and Sasai, N. (2010). Dynamic assignment and maintenance of positional identity in the ventral neural tube by the morphogen sonic hedgehog. *PLoS Biol.* **8**, e1000382.

Djenoune, L., Khabou, H., Joubert, F., Quan, F. B., Nunes Figueiredo, S., Bodineau, L., Del Bene, F., Burcklé, C., Tostivint, H. and Wyart, C. (2014). Investigation of spinal cerebrospinal fluid-contacting neurons expressing PKD2L1: evidence for a conserved system from fish to primates. *Front. Neuroanat.* **8**, 26.

Dougherty, K. J., Zagoraiou, L., Satoh, D., Rozani, I., Doobar, S., Arber, S., Jessell, T. M. and Kiehn, O. (2013). Locomotor rhythm generation linked to the output of spinal shox2 excitatory interneurons. *Neuron* **80**, 920-933.

Ericson, J., Rashbass, P., Schedl, A., Brenner-Morton, S., Kawakami, A., van Heyningen, V., Jessell, T. M. and Briscoe, J. (1997). Pax6 controls progenitor cell identity and neuronal fate in response to graded Shh signaling. *Cell* **90**, 169-180.

Espósito, M. S., Piatti, V. C., Laplagne, D. A., Morgenstern, N. A., Ferrari, C. C., Pitossi, F. J. and Schinder, A. F. (2005). Neuronal differentiation in the adult hippocampus recapitulates embryonic development. *J. Neurosci.* **25**, 10074-10086.

Fidelin, K., Djenoune, L., Stokes, C., Prendergast, A., Gomez, J., Baradel, A., Del Bene, F. and Wyart, C. (2015). State-dependent modulation of locomotion by GABAergic spinal sensory neurons. *Curr. Biol.* **25**, 3035-3047.

Francius, C., Harris, A., Rucchin, V., Hendricks, T. J., Stam, F. J., Barber, M., Kurek, D., Grosveld, F. G., Pierani, A., Goulding, M. et al. (2013). Identification of multiple subsets of ventral interneurons and differential distribution along the rostrocaudal axis of the developing spinal cord. *PLoS ONE* **8**, e70325.

Fu, H., Qi, Y., Tan, M., Cai, J., Hu, X., Liu, Z., Jensen, J. and Qiu, M. (2003). Molecular mapping of the origin of postnatal spinal cord ependymal cells: evidence that adult ependymal cells are derived from Nkx6.1+ ventral neural progenitor cells. *J. Comp. Neurol.* **456**, 237-244.

Gosgnach, S., Lanuza, G. M., Butt, S. J. B., Saueressig, H., Zhang, Y., Velasquez, T., Riethmacher, D., Callaway, E. M., Kiehn, O. and Goulding, M. (2006). V1 spinal neurons regulate the speed of vertebrate locomotor outputs. *Nature* **440**, 215-219.

Goulding, M. (2009). Circuits controlling vertebrate locomotion: moving in a new direction. *Nat. Rev. Neurosci.* **10**, 507-518.

Gross, M. K., Dottori, M. and Goulding, M. (2002). Lbx1 specifies somatosensory association interneurons in the dorsal spinal cord. *Neuron* **34**, 535-549.

Hochstim, C., Deneen, B., Lukaszewicz, A., Zhou, Q. and Anderson, D. J. (2008). Identification of positionally distinct astrocyte subtypes whose identities are specified by a homeodomain code. *Cell* **133**, 510-522.

Holz, A., Kollmus, H., Ryge, J., Niederkofler, V., Dias, J., Ericson, J., Stoeckli, E. T., Kiehn, O. and Arnold, H.-H. (2010). The transcription factors Nkx2.2 and Nkx2.9 play a novel role in floor plate development and commissural axon guidance. *Development* **137**, 4249-4260.

Huang, A. L., Chen, X., Hoon, M. A., Chandrashekar, J., Guo, W., Tränkner, D., Ryba, N. J. P. and Zuker, C. S. (2006). The cells and logic for mammalian sour taste detection. *Nature* **442**, 934-938.

Huang, P., Xiong, F., Megason, S. G. and Schier, A. F. (2012). Attenuation of Notch and Hedgehog signaling is required for fate specification in the spinal cord. *PLoS Genet.* **8**, e1002762.

Ishimaru, Y., Inada, H., Kubota, M., Zhuang, H., Tominaga, M. and Matsunami, H. (2006). Transient receptor potential family members PKD1L3 and PKD2L1 form a candidate sour taste receptor. *Proc. Natl. Acad. Sci. USA* **103**, 12569-12574.

Jalalvand, E., Robertson, B., Wallén, P., Hill, R. H. and Grillner, S. (2014). Laterally projecting cerebrospinal fluid-contacting cells in the lamprey spinal cord are of two distinct types. *J. Comp. Neurol.* **522**, 1753-1768.

Jessell, T. M. (2000). Neuronal specification in the spinal cord: inductive signals and transcriptional codes. *Nat. Rev. Genet.* **1**, 20-29.

Joshi, K., Lee, S., Lee, B., Lee, J. W. and Lee, S.-K. (2009). LMO4 controls the balance between excitatory and inhibitory spinal V2 interneurons. *Neuron* **61**, 839-851.

Karunaratne, A., Hargrave, M., Poh, A. and Yamada, T. (2002). GATA proteins identify a novel ventral interneuron subclass in the developing chick spinal cord. *Dev. Biol.* **249**, 30-43.

Kimura, Y., Satou, C. and Higashijima, S.-i. (2008). V2a and V2b neurons are generated by the final divisions of pair-producing progenitors in the zebrafish spinal cord. *Development* **135**, 3001-3005.

Kirby, B. B., Takada, N., Latimer, A. J., Shin, J., Carney, T. J., Kelsh, R. N. and Appel, B. (2006). In vivo time-lapse imaging shows dynamic oligodendrocyte progenitor behavior during zebrafish development. *Nat. Neurosci.* **9**, 1506-1511.

Kútna, V., Ševc, J., Gombalová, Z., Matiašová, A. and Daxnerová, Z. (2014). Enigmatic cerebrospinal fluid-contacting neurons arise even after the termination of neurogenesis in the rat spinal cord during embryonic development and retain their immature-like characteristics until adulthood. *Acta Histochem.* **116**, 278-285.

Lanuza, G. M., Gosgnach, S., Pierani, A., Jessell, T. M. and Goulding, M. (2004). Genetic identification of spinal interneurons that coordinate left-right locomotor activity necessary for walking movements. *Neuron* **42**, 375-386.

Laplagne, D. A., Zylberman, V., Ainciart, N., Steward, M. W., Sciutto, E., Fossati, C. A. and Goldbaum, F. A. (2004). Engineering of a polymeric bacterial protein as a scaffold for the multiple display of peptides. *Proteins* **57**, 820-828.

Lek, M., Dias, J. M., Marklund, U., Uhde, C. W., Kurdija, S., Lei, Q., Sussel, L., Rubenstein, J. L., Matise, M. P., Arnold, H.-H. et al. (2010). A homeodomain feedback circuit underlies step-function interpretation of a Shh morphogen gradient during ventral neural patterning. *Development* **137**, 4051-4060.

Li, S., Mo, Z., Yang, X., Price, S. M., Shen, M. M. and Xiang, M. (2004). Foxn4 controls the genesis of amacrine and horizontal cells by retinal progenitors. *Neuron* **43**, 795-807.

Li, S., Misra, K., Matise, M. P. and Xiang, M. (2005). Foxn4 acts synergistically with Mash1 to specify subtype identity of V2 interneurons in the spinal cord. *Proc. Natl. Acad. Sci. USA* **102**, 10688-10693.

Lu, Q. R., Sun, T., Zhu, Z., Ma, N., Garcia, M., Stiles, C. D. and Rowitch, D. H. (2002). Common developmental requirement for Olig function indicates a motor neuron/oligodendrocyte connection. *Cell* **109**, 75-86.

Lundfald, L., Restrepo, C. E., Butt, S. J. B., Peng, C.-Y., Droho, S., Endo, T., Zeilhofer, H. U., Sharma, K. and Kiehn, O. (2007). Phenotype of V2-derived interneurons and their relationship to the axon guidance molecule EphA4 in the developing mouse spinal cord. *Eur. J. Neurosci.* **26**, 2989-3002.

Madisen, L., Zwingman, T. A., Sunkin, S. M., Oh, S. W., Zariwala, H. A., Gu, H., Ng, L. L., Palmiter, R. D., Hawrylycz, M. J., Jones, A. R. et al. (2010). A robust and high-throughput Cre reporting and characterization system for the whole mouse brain. *Nat. Neurosci.* **13**, 133-140.

Mao, X., Fujiwara, Y., Chapdelaine, A., Yang, H. and Orkin, S. H. (2001). Activation of EGFP expression by Cre-mediated excision in a new ROSA26 reporter mouse strain. *Blood* **97**, 324-326.

Marichal, N., Garcia, G., Radmilovich, M., Trujillo-Cenoz, O. and Russo, R. E. (2009). Enigmatic central canal contacting cells: immature neurons in "standby mode"? *J. Neurosci.* **29**, 10010-10024.

Marichal, N., García, G., Radmilovich, M., Trujillo-Cenóz, O. and Russo, R. E. (2012). Spatial domains of progenitor-like cells and functional complexity of a stem cell niche in the neonatal rat spinal cord. *Stem Cells* **30**, 2020-2031.

McKinney, M. and McNamara, K. J. (1991). *Heterochrony: The Evolution of Ontogeny*. New York: Springer US.

Meletis, K., Barnabé-Heider, F., Carlén, M., Evergren, E., Tomilin, N., Shupliakov, O. and Frisén, J. (2008). Spinal cord injury reveals multilineage differentiation of ependymal cells. *PLoS Biol.* **6**, e182.

Orts-Del'Immagine, A., Wanaverbecq, N., Tardivel, C., Tillement, V., Dallaporta, M. and Trouslard, J. (2012). Properties of subependymal cerebrospinal fluid contacting neurones in the dorsal vagal complex of the mouse brainstem. *J. Physiol.* **590**, 3719-3741.

Orts-Del'Immagine, A., Kastner, A., Tillement, V., Tardivel, C., Trouslard, J. and Wanaverbecq, N. (2014). Morphology, distribution and phenotype of polycystin kidney disease 2-like 1-positive cerebrospinal fluid contacting neurons in the brainstem of adult mice. *PLoS ONE* **9**, e87748.

Orts Del'Immagine, A., Seddik, R., Tell, F., Airault, C., Er-Raoui, G., Najimi, M., Trouslard, J. and Wanaverbecq, N. (2016). A single polycystic kidney disease 2-like 1 channel opening acts as a spike generator in cerebrospinal fluid-contacting neurons of adult mouse brainstem. *Neuropharmacology.* **101**, 549-565.

Panayi, H., Panayiotou, E., Orford, M., Genethliou, N., Mean, R., Lapathitis, G., Li, S., Xiang, M., Kessaris, N., Richardson, W. D. et al. (2010). Sox1 is required for the specification of a novel p2-derived interneuron subtype in the mouse ventral spinal cord. *J. Neurosci.* **30**, 12274-12280.

Panayiotou, E., Panayi, E., Lapathitis, G., Francius, C., Clotman, F., Kessaris, N., Richardson, W. D. and Malas, S. (2013). Pax6 is expressed in subsets of V0 and V2 interneurons in the ventral spinal cord in mice. *Gene Expr. Patterns* **13**, 328-334.

Park, H.-C., Shin, J. and Appel, B. (2004). Spatial and temporal regulation of ventral spinal cord precursor specification by Hedgehog signaling. *Development* **131**, 5959-5969.
Peng, C.-Y., Yajima, H., Burns, C. E., Zon, L. I., Sisodia, S. S., Pfaff, S. L. and Sharma, K. (2007). Notch and MAML signaling drives Scl-dependent interneuron diversity in the spinal cord. *Neuron* **53**, 813-827.
Pierani, A., Moran-Rivard, L., Sunshine, M. J., Littman, D. R., Goulding, M. and Jessell, T. M. (2001). Control of interneuron fate in the developing spinal cord by the progenitor homeodomain protein Dbx1. *Neuron* **29**, 367-384.
Reali, C., Fernández, A., Radmilovich, M., Trujillo-Cenóz, O. and Russo, R. E. (2011). GABAergic signalling in a neurogenic niche of the turtle spinal cord. *J. Physiol.* **589**, 5633-5647.
Rocha, S. F., Lopes, S. S., Gossler, A. and Henrique, D. (2009). Dll1 and Dll4 function sequentially in the retina and pV2 domain of the spinal cord to regulate neurogenesis and create cell diversity. *Dev. Biol.* **328**, 54-65.
Rowitch, D. H. (2004). Glial specification in the vertebrate neural tube. *Nat. Rev. Neurosci.* **5**, 409-419.
Rowitch, D. H. and Kriegstein, A. R. (2010). Developmental genetics of vertebrate glial-cell specification. *Nature* **468**, 214-222.
Sabourin, J.-C., Ackema, K. B., Ohayon, D., Guichet, P.-O., Perrin, F. E., Garces, A., Ripoll, C., Charité, J., Simonneau, L., Kettenmann, H. et al. (2009). A mesenchymal-like ZEB1(+) niche harbors dorsal radial glial fibrillary acidic protein-positive stem cells in the spinal cord. *Stem Cells* **27**, 2722-2733.
Sapir, T., Geiman, E. J., Wang, Z., Velasquez, T., Mitsui, S., Yoshihara, Y., Frank, E., Alvarez, F. J. and Goulding, M. (2004). Pax6 and engrailed 1 regulate two distinct aspects of renshaw cell development. *J. Neurosci.* **24**, 1255-1264.
Schäfer, M., Kinzel, D. and Winkler, C. (2007). Discontinuous organization and specification of the lateral floor plate in zebrafish. *Dev. Biol.* **301**, 117-129.
Semmo, M., Köttgen, M. and Hofherr, A. (2014). The TRPP subfamily and polycystin-1 proteins. *Handb. Exp. Pharmacol.* **222**, 675-711.
Shin, J., Poling, J., Park, H.-C. and Appel, B. (2007). Notch signaling regulates neural precursor allocation and binary neuronal fate decisions in zebrafish. *Development* **134**, 1911-1920.
Smith, K. K. (2003). Time's arrow: heterochrony and the evolution of development. *Int. J. Dev. Biol.* **47**, 613-621.
Spassky, N., Merkle, F. T., Flames, N., Tramontin, A. D., Garcia-Verdugo, J. M. and Alvarez-Buylla, A. (2005). Adult ependymal cells are postmitotic and are derived from radial glial cells during embryogenesis. *J. Neurosci.* **25**, 10-18.
Stam, F. J., Hendricks, T. J., Zhang, J., Geiman, E. J., Francius, C., Labosky, P. A., Clotman, F. and Goulding, M. (2012). Renshaw cell interneuron specialization is controlled by a temporally restricted transcription factor program. *Development* **139**, 179-190.
Stoeckel, M.-E., Uhl-Bronner, S., Hugel, S., Veinante, P., Klein, M.-J., Mutterer, J., Freund-Mercier, M.-J. and Schlichter, R. (2003). Cerebrospinal fluid-contacting neurons in the rat spinal cord, a gamma-aminobutyric acidergic system expressing the P2X2 subunit of purinergic receptors, PSA-NCAM, and GAP-43 immunoreactivities: light and electron microscopic study. *J. Comp. Neurol.* **457**, 159-174.
Strähle, U., Lam, C. S., Ertzer, R. and Rastegar, S. (2004). Vertebrate floor-plate specification: variations on common themes. *Trends Genet.* **20**, 155-162.
Suzuki, N., Ohneda, O., Minegishi, N., Nishikawa, M., Ohta, T., Takahashi, S., Engel, J. D. and Yamamoto, M. (2006). Combinatorial Gata2 and Sca1 expression defines hematopoietic stem cells in the bone marrow niche. *Proc. Natl. Acad. Sci. USA* **103**, 2202-2207.
Tamamaki, N., Yanagawa, Y., Tomioka, R., Miyazaki, J.-I., Obata, K. and Kaneko, T. (2003). Green fluorescent protein expression and colocalization with calretinin, parvalbumin, and somatostatin in the GAD67-GFP knock-in mouse. *J. Comp. Neurol.* **467**, 60-79.
Taniguchi, H., He, M., Wu, P., Kim, S., Paik, R., Sugino, K., Kvitsiani, D., Fu, Y., Lu, J., Lin, Y. et al. (2011). A resource of Cre driver lines for genetic targeting of GABAergic neurons in cerebral cortex. *Neuron* **71**, 995-1013.
Temple, S. (2001). The development of neural stem cells. *Nature* **414**, 112-117.
Tsai, H.-H., Li, H., Fuentealba, L. C., Molofsky, A. V., Taveira-Marques, R., Zhuang, H., Tenney, A., Murnen, A. T., Fancy, S. P. J., Merkle, F. et al. (2012). Regional astrocyte allocation regulates CNS synaptogenesis and repair. *Science* **337**, 358-362.
Vallstedt, A., Klos, J. M. and Ericson, J. (2005). Multiple dorsoventral origins of oligodendrocyte generation in the spinal cord and hindbrain. *Neuron* **45**, 55-67.
van Doorninck, J. H., van Der Wees, J., Karis, A., Goedknegt, E., Engel, J. D., Coesmans, M., Rutteman, M., Grosveld, F. and De Zeeuw, C. I. (1999). GATA-3 is involved in the development of serotonergic neurons in the caudal raphe nuclei. *J. Neurosci.* **19**, RC12.
Vigh, B. and Vigh-Teichmann, I. (1971). Structure of the medullo-spinal liquor contacting neuronal system. *Acta Biol. Acad. Sci. Hung.* **22**, 227-243.
Vigh, B. and Vigh-Teichmann, I. (1998). Actual problems of the cerebrospinal fluid-contacting neurons. *Microsc. Res. Tech.* **41**, 57-83.
Vigh, B., Vigh-Teichmann, I. and Aros, B. (1977). Special dendritic and axonal endings formed by the cerebrospinal fluid contacting neurons of the spinal cord. *Cell Tissue Res.* **183**, 541-552.
Vigh, B., Vigh-Teichmann, I., Manzano e Silva, M. J. and van den Pol, A. N. (1983). Cerebrospinal fluid-contacting neurons of the central canal and terminal ventricle in various vertebrates. *Cell Tissue Res.* **231**, 615-621.
Vigh, B., Manzano e Silva, M. J., Frank, C. L., Vincze, C., Czirok, S. J., Szabo, A., Lukats, A. and Szel, A. (2004). The system of cerebrospinal fluid-contacting neurons. Its supposed role in the nonsynaptic signal transmission of the brain. *Histol. Histopathol.* **19**, 607-628.
Wyart, C., Del Bene, F., Warp, E., Scott, E. K., Trauner, D., Baier, H. and Isacoff, E. Y. (2009). Optogenetic dissection of a behavioural module in the vertebrate spinal cord. *Nature* **461**, 407-410.
Yang, L., Rastegar, S. and Strahle, U. (2010). Regulatory interactions specifying Kolmer-Agduhr interneurons. *Development* **137**, 2713-2722.
Yeo, S.-Y. and Chitnis, A. B. (2007). Jagged-mediated Notch signaling maintains proliferating neural progenitors and regulates cell diversity in the ventral spinal cord. *Proc. Natl. Acad. Sci. USA* **104**, 5913-5918.
Yu, K., McGlynn, S. and Matise, M. P. (2013). Floor plate-derived sonic hedgehog regulates glial and ependymal cell fates in the developing spinal cord. *Development* **140**, 1594-1604.
Zhang, Z.-w. (2004). Maturation of layer V pyramidal neurons in the rat prefrontal cortex: intrinsic properties and synaptic function. *J. Neurophysiol.* **91**, 1171-1182.
Zhang, Y., Narayan, S., Geiman, E., Lanuza, G. M., Velasquez, T., Shanks, B., Akay, T., Dyck, J., Pearson, K., Gosgnach, S. et al. (2008). V3 spinal neurons establish a robust and balanced locomotor rhythm during walking. *Neuron* **60**, 84-96.
Zhang, J., Lanuza, G. M., Britz, O., Wang, Z., Siembab, V. C., Zhang, Y., Velasquez, T., Alvarez, F. J., Frank, E. and Goulding, M. (2014). V1 and v2b interneurons secure the alternating flexor-extensor motor activity mice require for limbed locomotion. *Neuron* **82**, 138-150.
Zhou, Q. and Anderson, D. J. (2002). The bHLH transcription factors OLIG2 and OLIG1 couple neuronal and glial subtype specification. *Cell* **109**, 61-73.
Zhou, Y., Yamamoto, M. and Engel, J. D. (2000). GATA2 is required for the generation of V2 interneurons. *Development* **127**, 3829-3838.
Ziskind-Conhaim, L. (1988). Electrical properties of motoneurons in the spinal cord of rat embryos. *Dev. Biol.* **128**, 21-29.